Department of Precision and Microsystems Engineering

**Indirect sensing method for contact location and force
in a compliant finger**

Rens de Rooij
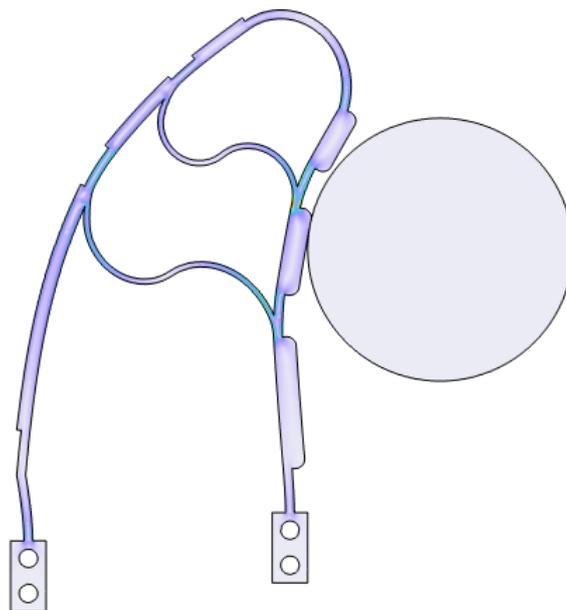
TUDelft

Preface

This thesis concludes my master Mechanical Engineering and thereby my time as a student at the faculty 3mE of the Delft University of Technology. The final project was a great way to combine the theoretical knowledge gained during the studies with a practical application.

I would like to thank my supervisors Ad Huisjes and Just Herder for their guidance and valuable feedback during this graduation project. I want to thank my fellow students from the gripper research group as well for their feedback during the weekly meetings. Furthermore, I would like to thank the people from the 3mE meetshop and the PME lab for their help with installing sensors, constructing an experimental set-up, and performing the measurements. I would like to thank my friends for providing me with the necessary distractions in the form of coffee breaks, bike rides, and countless drinks and lastly, I would like to thank my family for their support.

Rens de Rooij
Delft, January 2023

Contents

Chapter 1

Introduction

In order to deal with a growing worldwide food demand and increasing labor shortages, automation in the agri-food industry is required. An important aspect of this automation is developing robotic grippers that are capable of handling food products. Due to the fragile and deformable nature of these products, and the high demands on quality in the food industry, grippers should handle the products with great care to prevent damage. Compliant and underactuated grippers passively conform to the shape of the grasped object due to the design of their structure, thereby improving the gripper performance for this application. At the same time, the passive structure induces uncertainty about the stance of the compliant fingers. For this reason, the addition of sensing to robotic grippers can present new possibilities to take away this uncertainty and improve the grasping of natural products. This thesis focuses on embedding sensors onto robotic grippers, whereby a sensing method is developed that is able to indirectly measure contact position and contact forces in a compliant finger.

1.1   Research objectives

To investigate how the addition of sensing can help improve robotic grippers, it is relevant to first identify which gripper principles can be combined with which sensing methods to provide useful measurements. Furthermore, the challenges for embedding sensors in grippers need to be analyzed, with the application in the agri-food industry in mind. The first part of the research consists of a literature study that aims to address these objectives.

The analysis of grippers and sensing methods results in two measurable quantities of interest: contact location and contact force. The contact location provides insight into the gripper-object interaction, whereas the contact force is an important quantity for grasping, as it determines the stability of the grasp and the impact of the gripper on the object. In addition, compliant grippers are identified as suitable grippers, due to their predictable force-deformation behavior and promise in the agri-food application. This leads to the main research question of this thesis: can we estimate the contact location and contact force between a compliant finger and an object indirectly by measuring the strain inside the structure? Hereby, the contact location estimate should be able to distinguish between contacting phalanges of the compliant finger, and the contact force should be accurate in order of magnitude of several newtons. In addition, the indirect sensing method will aim to minimize the impact of the sensors on the gripper performance in terms of mobility of the gripper and required actuation force.

1.2 Thesis outline

Chapter 2 presents the literature study into the combination of gripper principles and sensing methods. It also describes the main challenges for embedding sensors in robotic grippers. In chapter 3 the main research of this thesis is presented in the form of a scientific paper, addressing the development of an indirect sensing method for a compliant finger, whereby contact location and contact forces are estimated using strain measurement. Chapter 4 describes an alternative method for determining the contact forces. In contrast to chapter 3, where the forces are derived using the results of a Finite Element Analysis (FEA), in this chapter the forces are determined through calibration. Chapter 5 provides a critical discussion of practical insights that are gained throughout the project, elaborating on the discussion part of the research paper. Finally, chapter 6 presents the conclusions of the thesis. The appendices provide a more detailed overview of the experimental set-up (appendix A) and the Finite Element Analysis in COMSOL Multiphysics (appendix B).

Chapter 2

Literature study

2.1 Introduction

One of the problems that humankind is encountering currently, is providing all people with enough food. The worldwide population is rapidly growing and is expected to keep on growing for the foreseeable future. This results in a growing demand for food [1]. At the same time, there is an increasing labor shortage in agriculture [2]. To keep up with the growing food demand and overcome labor shortages, automation of certain processes in agriculture is needed. The number of robots in agriculture is growing, for example in the harvesting of fruits and vegetables [2][3][4], and the processing of food products [5]. However, the amount of automation in agriculture and food processing is lagging behind other industries, where automation is widely used. One of the most important challenges for robots handling food products is the fact that these products are deformable and should be handled with care to prevent damage. To overcome these challenges, new robotic grippers should be developed that can handle deformable and fragile natural products. For example, compliant and underactuated grippers passively conform to the shape of the grasped object due to the design of their structure, thereby improving the gripper performance for this application. The addition of sensing to robotic grippers can present new possibilities to obtain information during the grasping process and to further improve the grasping of natural products.

The natural inspiration for the robotic grippers is the human hand. The human hand is an amazingly versatile instrument, capable of handling very small and fragile objects up to large and heavy objects. The dexterity of the human hand is partly due to the 20 degrees of freedom in movement of the hand. Secondly, the dexterity can be attributed to the sense of touch in human hands: more than 17000 mechanoreceptors [6] provide the human hand with the possibility to accurately perceive the size, shape, and characteristics of an object that is grasped. Similarly, the application of sensors in robotic hands might increase the capabilities of these hands in the handling of objects like food products.

This leads to the research question for this literature review: which gripper principles can be combined with which sensing methods to provide useful measurements? To answer this research question, first, the gripper principles available in literature are evaluated in Section 2.2. Next up in Section 2.3, the sensors that are used in robotic grippers are investigated. To conclude the literature research, the combinations of certain gripper principles with certain sensing methods are evaluated. In addition, some of the challenges for applying sensors in robotic grippers are identified. The answer to the research question and the conclusions of the literature review lead to a project proposal for follow-up research.

2.2 Gripper principles

Over the course of the last 30 years, a wide variety of robotic grippers has been developed. These grippers show various designs, ranging from dexterous, human-like hands to vacuum suction cups. To provide a complete overview of the grippers described in literature, in this review a classification of the grippers will be presented. The grippers can be distinguished based on various characteristics like compliancy (rigid, compliant or soft), driving force (pneumatic, electric, magnetic) or gripper principle (actuated movement, controlled stiffness, controlled adhesion). The grippers will be subdivided, mainly based on gripper principles. Figure 2.1 shows an overview of this gripper classification, which is partly based on the classification of soft robotic grippers in [7].

The first and most important distinguishing feature shown in figure 2.1 is the gripper principle: grippers use either actuated movement, controlled stiffness or controlled adhesion to grasp objects.

Robotic Grippers

- Gripping by actuated movement
  - Passive structure with external motors
    - Rigid structure
      - 2 fingers
      - 3 or more fingers
    - Compliant structure
      - Fin-ray structure
      - Compliant fingers
  - Fluidic elastomer actuators
  - Electroactive polymers
    - Dielectric elastomer actuators
    - Ionic polymer-metal composites
  - Shape memory materials
- Gripping using controlled stiffness
  - Granular jamming
  - Low-melting point alloys
  - Electro/Magneto rheological fluid
  - Shape memory materials
- Gripping using controlled adhesion
  - Electro adhesion
  - Dry adhesion (Gecko)
  - Vacuum

Figure 2.1: Gripper classification overview

Gripping by actuated movement

The grippers based on actuated movement to grasp objects, use the movement of fingers or other elements for grasping. Two types of grasps can be obtained using this movement: a power grasp or a precision grasp [6]. Either the fingers envelop the object to form a power grasp, or the fingertips contact the object to form a precision grasp. A power grasp is characterized as a stable grasp, with a wide contact surface between the gripper and the object and capable of handling heavy objects. A precision grasp is less stable, as the contact surface is limited to the fingertips. This grasp is better suited for fragile objects, as the contact forces are usually low.

When considering the classification in figure 2.1, the first branch of the gripping by actuated movement grippers is the most extensively researched and most used type of gripper. These grippers consist of a passive structure that is actuated by an external force. The passive structure often resembles a hand, with a varying number of fingers and finger structures. The rigid grippers consist of rigid elements, linked together through rotational joints. The grippers are mostly actuated using electric motors in the joints, tendons running through the fingers, or motors with a gearbox transmission to allow finger movement. A wide range of examples of this type of grippers can be found in [6].

In contrast to the rigid links and rotational joints used in rigid grippers, compliant grippers use flexible joints to achieve finger movement and are often constructed using deformable materials. One of the most commonly used compliant fingers is the so-called fin-ray gripper, as shown in figure 2.2a. The fin-ray gripper is already applied in some agricultural robots [8].

Besides the fin-ray structured finger, there is a whole range of compliant fingers that are used for grasping, varying from rigid links connected with flexible joints to completely deformable finger structures. These compliant fingers also differ in the motion path followed by the fingers. Widely used design techniques for compliant structures include topology optimization, whereas for fabrication 3D printing is a common technique. An example of such a gripper is shown in
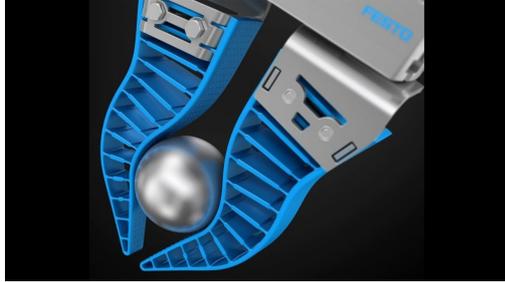
(a) Fin-ray gripper designed by Festo [9]   (b) 3D printed compliant gripper structure [10]
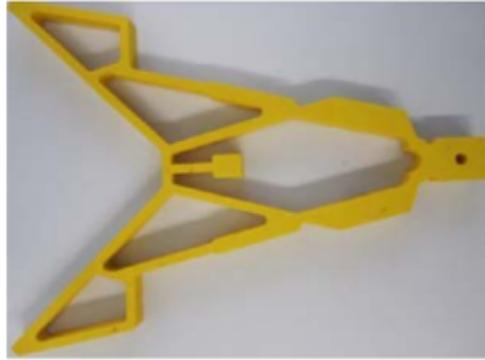
Figure 2.2: Compliant grippers

figure 2.2b. Other examples can be found in [11], [12], [13] and [14].

A relatively new branch of robotics that is rapidly developing is soft robotics [15][16]. In soft robotics, robots are constructed using soft and stretchable materials like rubber, to create functionalities that rigid grippers cannot obtain and to resemble natural tissues. Soft robotics is increasingly applied in grippers, and one of the most important techniques uses Fluidic Elastomer Actuators (FEAs). FEAs are constructed of rubbery materials and are actuated by pumping a fluid into the actuator. Due to the incoming fluid and the structure of the FEA, a prescribed movement is followed. These actuators can be used to perform finger movements, and thereby compose a gripper. An example of such a soft gripper is presented in [17], and the finger used in this gripper is shown in figure 2.3. Due to the structure, the finger will bend over the lower part when fluid is pumped in. Through this bending, the finger can form around an object. Further references for the use of FEAs for grasping are: [18] and [19].
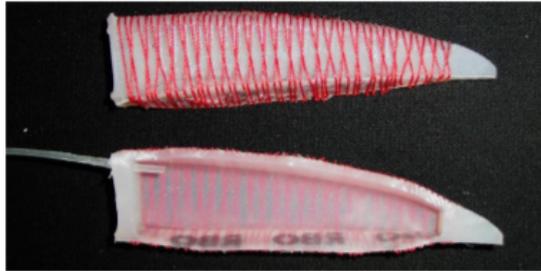
Figure 2.3: Fluid Elastomer Actuator finger [17]

Another type of actuated movement gripper uses electroactive polymers to achieve gripping movements. These grippers utilize the properties of electroactive polymers, which show deformation under the application of an electric voltage. By proper design, this deformation can be converted into a gripping movement. For dielectric elastomer actuators, this is achieved by placing an elastic material in between two compliant electrodes. When a voltage is applied over the electrodes, the electrostatic attraction between the two electrodes, resulting from the voltage, causes a deformation of the compliant electrodes and the elastomer in between. An ionic polymer-metal composite also has a layered structure, comprised of two thin metal plates with

an ionic polymer in between. An applied voltage over the metal plates results in ion movement within the ionic polymer, which in turn causes a deformation of the entire structure. The deformation can be utilized for a gripping movement.

Gripping by actuated movement can be achieved by shape memory materials as well. These materials can be deformed from their original shape, and return to this original shape when the material is heated. This principle can be achieved by certain alloys and some polymers, due to the internal structure of the material. [20] and [21] show examples of robotic grippers where the shape change of shape memory materials is used to actuate the design.

Gripping using controlled stiffness

The next main branch in the gripper classification in figure 2.1 is gripping using controlled stiffness. This type of gripper uses the material properties of certain elements: these materials can undergo a large change in stiffness under the right circumstances. This change in stiffness is utilized in the grasping of objects. When the material stiffness of a gripper is low, it can be easily conformed to the shape of an object. Retaining the current gripper shape, the stiffness is increased such that the gripper is almost rigid. The rigid gripper is able to hold the object to which shape it conforms.

One of the grippers that use this principle to grasp objects is presented in [22] and shown in figure 2.4. This gripper consists of an elastic bag filled with granular material. Under normal conditions, this elastic bag can be pressed on an object, whereby it conforms to the shape of the object. When a vacuum is applied to the elastic bag, the granular material is pressed together, which results in a high rigidity while remaining conformed to the object's shape. As shown in the figure, the object can be picked up.
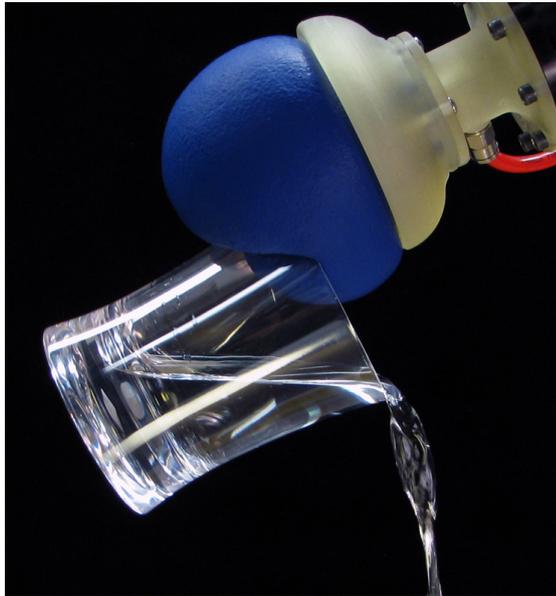
Figure 2.4: Gripper based on the jamming of granular material [22]

Other types of materials that can be utilized for the purpose of gripping using controlled stiffness are low melting point alloys. As is in the name, these alloys can change from solid to liquid state at a relatively low temperature. The large difference in stiffness between the solid and liquid

state is exploited. Electro/magnetorheological fluids show a large change in viscosity of the fluid upon application of either an electric or a magnetic field. Shape memory materials not only change their shape, as explained in the previous section, but also change their stiffness under the right circumstances. Especially shape memory polymers display this characteristic. The aforementioned materials are incorporated in complex finger and gripper designs in order to use the change in stiffness for gripping behavior.

Gripping using controlled adhesion

The last main branch of gripping principles from figure 2.1, comprises the grippers that use controlled adhesion to pick up objects. This type of gripper exploits the high surface forces that can be accomplished between a gripper and an object under certain circumstances. The main methods to obtain controlled adhesion are by using electro-adhesion, dry adhesion, or a vacuum gripper.

Electro-adhesion is the surface force between two objects due to electrostatic forces. Electrostatic or Coulomb forces are the forces between electric charges. When the surface of the gripper has an opposite electric charge to the surface of the object, electro-adhesion can be used to pick up the object. This difference in charge between the surfaces is induced by applying an electric field. Dry adhesion grippers use Van Der Waals forces to achieve a high surface force. Van Der Waals forces are the mutual forces between molecules or atoms. Normally these microscopic forces are far from sufficient to pick up macroscopic objects, but high surface forces can be achieved for specifically structured surfaces. Geckos are able to climb and hang on to surfaces using their specific foot structure. On a microscale, the foot structure consists of millions of hair-like fibers, which in turn branch out into even smaller structures. When the feet touch a surface, a very large number of these nanostructures come into contact with the surface. Thereby the surface area is vastly increased, allowing for higher Van Der Waals forces sufficient to support the Gecko's body weight. Gecko feet serve as inspiration for several dry adhesion grippers. An example is shown in figure 2.5 and described extensively in [23]. The gripper in this article exists of a flexible, inflatable membrane. The membrane surface is equipped with a large number of microfibers, as displayed on the right in figure 2.5. Similar to the Gecko feet, the microfibers increase the contact surface, and thereby the adhesion forces between gripper and object. When picking up an object, the membrane is not inflated and conforms to the shape of the object with a large contact area. To release the object again, the membrane is inflated, decreasing the contact area and the number of fibers in contact with the object. When the number of microfibers in contact is sufficiently low such that the Van Der Waals forces are lower than the object weight, the object is released.
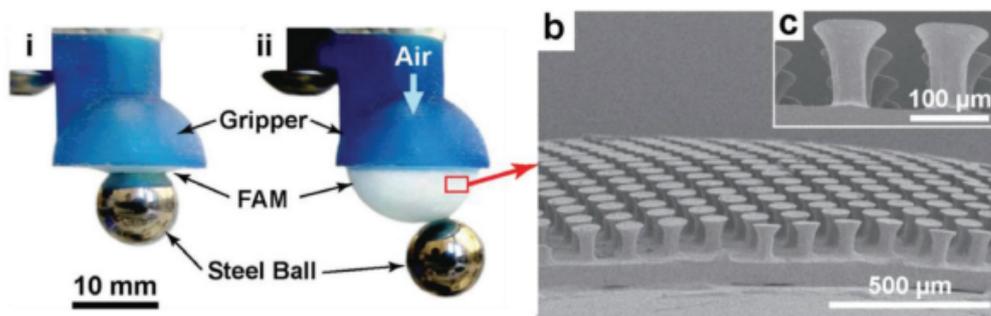
Figure 2.5: Gecko inspired dry adhesion gripper [23]

One of the most widely used methods for gripping in industry is using a vacuum. A vacuum suction cup, depicted in figure 2.6, is brought into contact with the object's surface. A vacuum is generated in the cup by sucking out the air within the cup. The result is that the pressure outside the cup is higher than within. The outside pressure provides the force to keep the object and cup in contact.

Figure 2.6: Vacuum suction cup by Festo [24]

2.3   Sensors in Grippers

Similar to the classification of grippers presented in the previous section, the sensors and sensing methods that can be used in robotic grippers are also ordered in an overview with different branches: figure 2.7. In this overview, the main sensing methods are distinguished equivalently to how we as humans perceive while grasping an object: namely based on vision, proprioception and tactile feedback. When grasping an object, we look at the object and our hand. We estimate distances based on visual feedback and move our hand accordingly toward the object. The second important aspect when grasping an object is the knowledge we have of the position of our hands and the forces in our muscles, called proprioception. Even without visual feedback, we know the position of our fingers, whether we are making an open hand or a fist. The last important sensing method we use while grasping an object is our sense of touch: based on the feedback from the tactile sensors in our skin we know when we touch an object, how much force we need to exert on the object to hold it, and when it starts to slip out of our hand.

For each of these natural sensing methods, equivalent artificial sensors exist that can be applied in robotics. In the upcoming section, these artificial sensors are discussed with an application in robotic grippers for food products in mind. For every possible sensor, the possible measurements and the placement when used in combination with a robotic gripper are discussed. The sensors that are introduced are deemed to provide some added value for usage in gripping food products. Besides introducing and explaining these sensors, they are also evaluated separately, with general advantages and disadvantages per sensor. Secondly, the possibilities and impossibilities of combining the sensor with certain grippers and gripper principles are discussed.

This review of the sensors is focused on the sensors that are applied within the robotic gripper: the end-effector. More sensors exist that can be placed on the base of the robot, on the robotic arm, or externally from the robot. These types of sensors are not considered in this review.
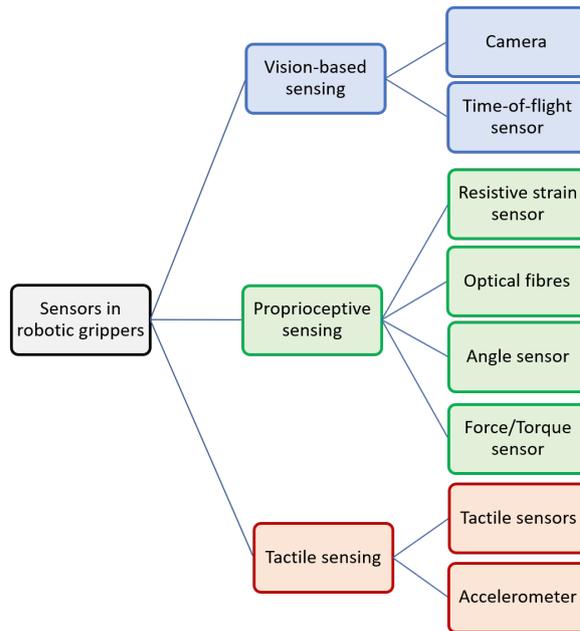
Figure 2.7: Sensor overview

Vision-based sensing

Camera

A camera is used for visual inspection of the gripper or object. As this is an evaluation of sensors on the end-effector, the camera in this case is mounted on the wrist of the gripper, a so-called eye-in-hand camera. Possible measurements performed using a camera are detection of the presence of an object, the color of an object, the deformation of either the gripper or the object, and slip detection. The color of the object can be an indication of the ripeness when considering fruits or vegetables. In [8], a camera is installed above the gripper in a pepper harvesting robot, shown in figure 2.8.

An advantage of a camera is the wide functionality it provides: it can be used for multiple measurements. Besides, it does not only perceive the object and the gripper, but also the environment, allowing for obstacle detection. However, these environmental factors like leaves or stems when considering a greenhouse environment, can also occlude the camera and thereby block the vision. A camera can be useful for every type of gripper in determining the presence of an object or object properties like color. When placement on the wrist is assumed though, for gripper principles like granular jamming and dry adhesion it is difficult to detect deformations and slip, as these grippers partially envelop objects.

Time-of-flight sensor

A time-of-flight(ToF) sensor is used to measure the distance of the sensor to an object. This measurement is based on the time between the emission of a signal and the return to the sensor after it is reflected by the object. This principle is depicted in figure 2.9. The ToF sensor can either be a simple sensor or a more advanced camera that can measure multiple distances in 3D. Similar to the normal camera, this sensor could be mounted on the wrist, above (or below) the
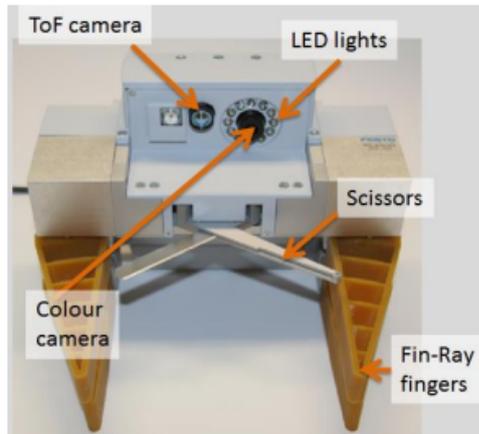
Figure 2.8: Pepper harvesting robot, including a camera and time-of-flight sensor mounted above the gripper [8]

end-effector. In the pepper harvesting robot in [8](figure 2.8), a time-of-flight camera is used in combination with a normal camera.
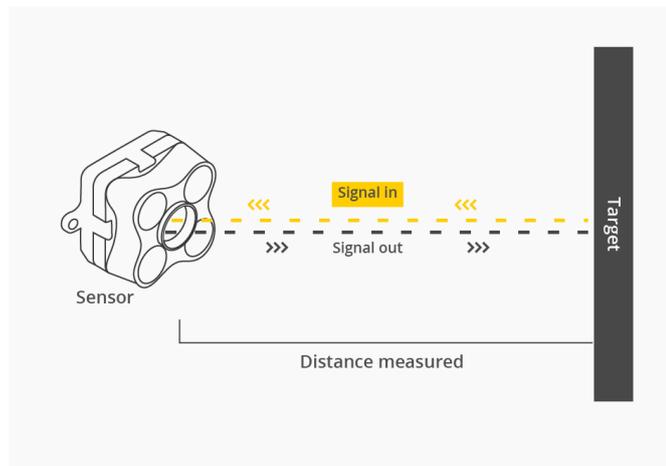
Figure 2.9: Time-of-flight sensor principle [25]

The most important advantage of a time-of-flight sensor is the fact that it provides a direct measurement of the distance between for example gripper and objects. Similar to a camera, occlusions can block vision. The time-of-flight sensor is especially useful for fingered grippers (rigid, compliant, and soft), where the placement of the object within the hand is crucial in obtaining a stable grasp. For principles like granular jamming, vacuum suction cups, or inflatable pockets the exact placement of the object in the gripper is less important, so a time-of-flight sensor will contribute less to increased gripper performance.

Proprioceptive sensing

Resistive strain sensor

A resistive strain sensor is used to measure the strain in flexible fingers or joints, whereby the resistance of the sensor changes upon bending (see figure 2.10). For entirely compliant and soft robotic hands or hands with flexible joints, this strain measure can be used to deduce the finger position, stance, and deformation. In turn, this stance and deformation could be a measure of the forces on the object. Examples of strain sensors used in grippers are provided in [18] and [19].

Figure 2.10: Simple resistive strain sensor

A resistive strain sensor can be internal, which is a great advantage in an environment that can disturb the measurements. In addition, calibration can be used to map the strain measure to other quantities such as force. A strain sensor can be combined with compliant or soft-fingered grippers, where the deformation of the fingers determines the hand position. For rigid fingers with flexible joints, it might be useful as well, but entirely rigid fingers hardly show strain. For principles like granular jamming and dry adhesion, the deformations are local and highly dependent on the object's shape and position with respect to the gripper, which makes it harder to extract useful data from a strain measurement.

Optical fibres

Optical fibers embedded in flexible fingers can be used to measure the curvature of these fingers. Optical fibers are used to guide light signals, whereby the fiber has a transmitting and a receiving end. A light signal is transmitted through the fibers and perceived at the receiving end. The received signal depends on the length and shape of the optical fiber. When embedded into a flexible finger, the perceived light signal changes based on the curvature of the finger, and is thereby a measure for this curvature. In a similar manner to the strain measurement of the resistive strain sensor, the curvature can be used to deduce other gripper information and quantities. [26] and [27] provide examples where the measurements of optical fibers in flexible fingers are linked to force and torque data, as well as shape, surface roughness and softness detection of objects. This is achieved by using techniques like calibration and machine learning. Figure 2.11 shows a detailed overview of how the researchers in [27] have integrated the optical fibers into a flexible finger.

Like the resistive strain sensor, the advantages of optical fibers include that they can be internal
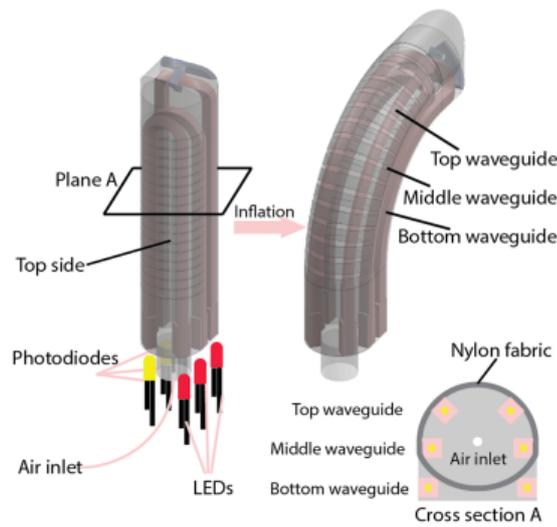
Figure 2.11: Detailed overview of optical fibers integrated into a soft robotic finger [27]

and that calibration allows for extracting more information based on curvature measurement. The application space for optical fibers is the same as for the resistive strain sensors: namely compliant and soft-fingered grippers, and possibly rigid fingers with flexible joints.

Angle sensor

An angle sensor, for example an encoder(figure 2.12) or potentiometer, is used to measure the angle of a joint of the gripper. For rigid or partially flexible grippers containing joints, the joint angle measure is a way to determine the gripper posture. As with the optical fibers and resistive strain sensor, further quantities can be derived from the gripper posture.

Figure 2.12: Rotary encoder [28]

Encoders are often built-in within robotic joints, so no separate sensor has to be acquired and installed. A challenge for the application of angle sensors is that for multi-phalanx fingers, every joint angle needs to be measured to determine hand posture. In contrast to the resistive strain

sensor and optical fibers, an encoder or potentiometer is not applicable for compliant or soft grippers, but only for grippers with rotational joints.

Force/Torque sensor

As is in the name, a force/torque sensor is used to measure forces and torques on the robotic hand, equivalent to how human perceive the forces and torques exerted by muscles. The sensor can be implemented in the wrist at the connection of the arm with the end-effector, as depicted in figure 2.13. Possible measurements with a force/torque sensor are the forces between the end-effector and environment, the object's weight, and in-hand displacements of the object.
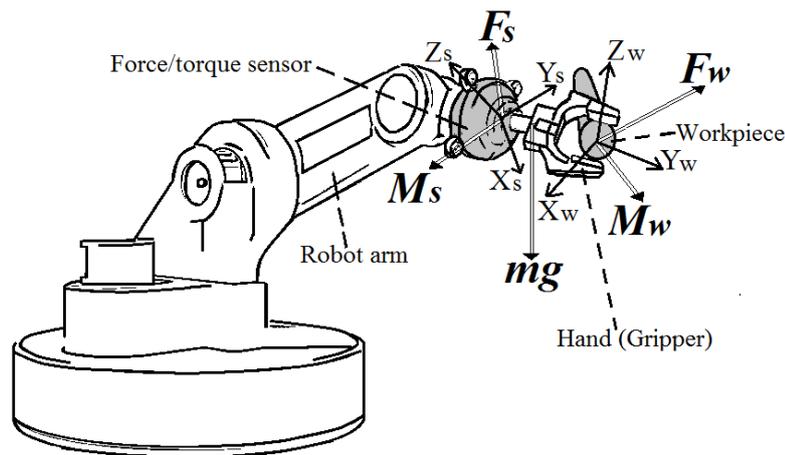
Figure 2.13: Implementation of a Force/Torque sensor in the wrist of a robot arm [29]

The most important added value of a force/torque sensor is in high-precision tasks like pick and place and insertion of objects, as it provides accurate measurements of the interactions with object and environment. A force/torque sensor is generally very expensive though. The implementation in-between the arm and end-effector can also pose problems, as both should be suitable to make this connection. A force/torque sensor is applicable to almost every gripper type, as measuring several aspects of the contact with the environment and objects can help in controlling the robot. However, for deformable or soft grippers, the deformations are not taken into account for the force/torque measurement. Therefore, the sensor is easier implemented on rigid grippers.

Tactile sensing

Tactile sensors

Tactile sensors are sensors at the finger or palm surface that measure contact with an object, comparable to the sensing elements in human fingers. There are several different principles to perform these measurements [30]. The most widely applied method uses an array of small contact sensors called tactels. Upon contact with an object, only the tactels that touch the object will see an increase in the measured value. When the whole array is visualized, the tactels in contact will show where the sensor is touching the object, mapping the contact surface. This is visualized in figure 2.14. In addition, most tactile arrays provide up to some point a relative measurement of the contact force. More advanced tactile sensors using vision are under development, whereby the

reflections of light signals are interpreted to deduce the contact area and force [31][32]. Besides placement on the finger and palm surface, tactile sensors could also be placed on the exterior of the gripper or arm to measure contact with the environment [33]. Other examples where tactile sensors are used in combination with gripping can be found in [34] and [35].
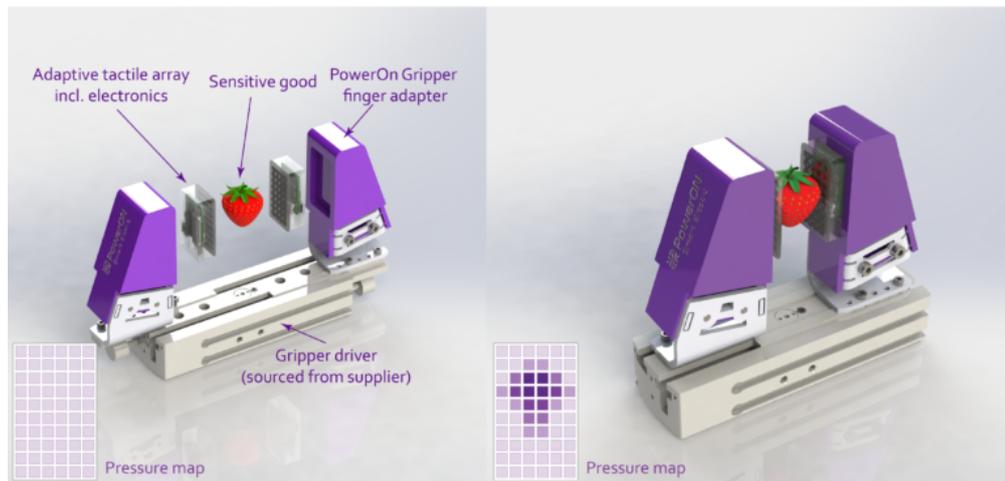
Figure 2.14: Tactile sensor showing a pressure map of the contact with an object [36]

An important advantage of tactile sensing is the fact that it can provide both a mapping of the contact surface as well as a contact force measurement. In addition, it is possible to perform slip detection using tactile sensors. Another advantage is the ability to improve the grasping of delicate objects by providing contact feedback. Disadvantages are that tactile sensors need to be placed at the gripper surface, which makes it not suitable for certain gripper types, and is sensitive to disturbances from the environment. Tactile sensors are mainly interesting for fingered grippers, as they can be implemented on the finger or palm surface. Especially for compliant grippers, tactile feedback of the contact with an object could provide added value, because due to the deformability, the exact contact location and forces are harder to model than with a rigid gripper. Further development in the field of flexible sensors is required to apply tactile sensing to soft or inflatable grippers. For dry adhesion grippers and suction cups, there is no application for tactile sensors on the end-effector, as the contact surface should not be covered with sensors for these principles to work.

Accelerometer

On a human finger, the fingerprint gives a little roughness to the finger surface. When an object slips over this surface, this causes vibrations, which are perceived by mechanoreceptors in the skin. Similarly, an accelerometer can perceive vibrations caused by slipping of an object over a robot finger surface and thereby detect slip. An accelerometer measures accelerations, often from the movement of a small, suspended mass, as shown in figure 2.15.
Using an accelerometer, slip can be detected in a very simple and straightforward manner. Also, the sensor can be implemented internally; it does not have to be placed directly at the surface. In contrast, external vibrations and disturbances are perceived as well, and filtering these out might prove challenging. The use of this sensor also induces a design requirement on the finger surface, as this should be somewhat rough in order to provide vibrations due to slip. The accelerometer can be combined with fingered grippers, either rigid or compliant, where it can be implemented
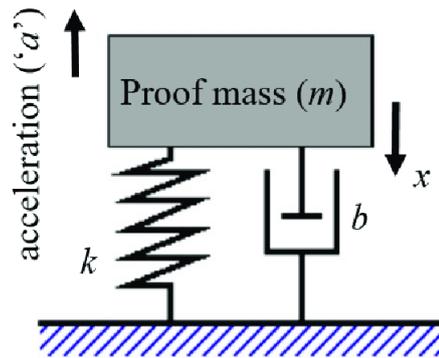
Figure 2.15: Accelerometer working principle: mass-spring-damper system, the deflection of the mass is a measure for the acceleration [37]

within the fingers. It will be challenging to implement it there, with limited space. However, for soft grippers and special principle grippers like granular jamming and dry adhesion, it will be even more difficult, as the implementation space is even more limited.

Input measurement

Besides the sensing methods and sensors in figure 2.7 and the previous sections, there is one other important measurement to take into account for gripping by actuated movement. When gripping by movement, the actuation input determines the behavior of the gripper. The input can therefore be a measure for the output force, output displacement, and hand position. Whether this input is a force, a displacement, or a pneumatic pressure, it provides important information on the gripper, certainly when combined with other sensor measurements.

2.4 Challenges for applying sensors in grippers

During this literature study, not only the robotic grippers in academic research were taken into account. Current robotics used in agricultural applications were also assessed to get a complete overview of the state of the art of agricultural robotics. The number of robots in industry is growing, and large agritech companies such as Priva and Ridder are investing in the development of robots used in harvesting and de-leafing. However, one of the things that stands out in the robots in industry is the lack of sensors within the end-effectors. To understand why there are no sensors applied within the end-effector, and thereby identify the challenges involved in this application, several companies and people involved in the agricultural robot development were contacted. The most important challenges following from these interviews, complemented with findings from literature [31], are presented in this section. These challenges are definitely applicable to this project as well, and therefore should be kept in mind in the follow-up research.

- Environmental factors lead to breakdown of the sensors: sensors are often relatively fragile electronic components, that can break down due to moisture, dirt, or chemicals. In the food industry, robots operate in environments where these factors are often present. In a greenhouse, there can be moisture in the air or coming from the plants, or dirt particles from the plants. The vegetables can be wet from condensation. In processing chicken parts, the gripper will be in contact with dirt and moisture from the chicken parts. Furthermore,

19

due to the high demands on hygiene in the food industry, the robots frequently need to get a thorough cleaning, often with corrosive cleaning chemicals.

- The sensors are difficult to install: the space for installation of sensors on the end-effector is often limited. The gripper surface is designed such that it is optimal for grasping objects, not for implementing sensors. Besides, many gripper designs are not suitable for the installation of sensors.

- The sensors are unnecessary to achieve the desired performance: often external cameras and controlled movements provide the robot with sufficient dexterity for the required functionality, without the need for sensors. In addition, robots in industry are often designed for one specific use case. The end-effector is designed and fine-tuned to make it suitable for this specific use case, whereby sensors are not necessary to achieve the desired performance.

- Protection from breakdown often goes at the expense of accuracy of measurements: when the sensors need to be protected from the factors mentioned above, this often comes with a decrease in accuracy. When adding a protective cover or installing the sensor within the gripper parts, the measurement is no longer directly on the gripper/object surface. These indirect measurements are either less accurate, need to take into account a transmission, or need calibration.

- Wiring, power supply, and circuitry make the end-effector design more complex.

- Costs: sensors, especially high-performance, are generally quite expensive.

2.5 Literature conclusions

Now that the most important gripper principles and sensing methods for those grippers are identified, and the most important challenges for applying sensors within the end-effector of a robot have been addressed, this knowledge has to be combined to answer the research question: which gripper principles can be combined with which sensing methods to provide useful measurements? To answer this research question, a table showing the combinations of gripper principles and sensors is provided, where the combinations are evaluated as well.

Combining gripper principles and sensors

To summarize the literature review and enable the comparison of different combinations of gripper principles with sensors, a table was created showing the most important gripper principles on the horizontal and the most important sensing methods on the vertical: figure 2.16. Not all gripper principles from the classification are taken into account, as some are still underdeveloped or not interesting for applications in agri-food. The accelerometer is left out of the table and replaced with slip sensing, as the accelerometer can only be used for slip sensing, but slip sensing can also be achieved by other sensors such as tactile sensors.

The black crosses in the table indicate that this combination of gripper and sensor has been researched before, whereas the red crosses indicate that a certain combination is either not feasible or not useful. The green crosses show a gap in the literature: judging from the literature these combinations are hardly researched before, but in my opinion, they might be interesting to investigate in further research. Lastly, the white spots in the table show the combinations that are not necessarily infeasible or not useful, but lay outside the scope of interest for this project. The table is created using the evaluation of the sensors in section 2.3. Furthermore, the application in agri-food is kept in mind.

The table shows that multiple sensors have already been applied for rigid grippers. Gripping using controlled adhesion proves much less suitable for the application of sensors, as the surface of the grippers does not allow the addition of sensors, and most sensor measurements do not provide added value for these gripper principles.

What further stands out from the table is that especially in the addition of sensors to compliant grippers there has not been much research in literature, whereas this might prove a very interesting application. In contrast to rigid grippers, where a lot of information on the finger positions and hand stance is known in advance from actuation input, there is uncertainty in the stance and position of compliant grippers due to the deformable nature of these grippers. The addition of sensors could provide valuable information to take away this uncertainty and help make the grippers more controllable. Furthermore, the force-deformation behavior of compliant grippers is predictable and can be modeled using a Finite Element Analysis.

Grippers / Sensors used	Gripping by actuation					Gripping using controlled stiffness	Gripping using controlled adhesion	
	Rigid 2 fingers	Rigid 3+ fingers	Compliant Fin-ray	Compliant Fingers	Soft Fluid elastomer actuation	Granular jamming	Dry adhesion (Gecko)	Vacuum
Vision-based sensing — Camera	x	x	x					x
Time of flight sensor	x	x	x	x	x			x
Pressure/force/torque sensor	x	x			x		x	x
Tactile sensing — Tactile sensors	x	x	x	x	x	x	x	x
Slip sensing	x	x	x	x		x	x	x
Resistive strain sensor	x	x	x	x	x		x	x
Optical fibres	x	x	x	x	x	x	x	x
Proprioceptive sensing — Angle sensor (encoder/potmeter)	x	x	x	x	x	x	x	x
Input measurement	x	x	x	x	x	x	x	x

Figure 2.16: Table showing the combinations of gripper principles and sensors

22

2.6 Project proposal

After extensively investigating the gripper principles and sensing methods that are available in literature, and evaluating the combinations of gripper principles with certain sensing methods, the proposal for the research project following this literature study can be presented. The following project goal is proposed:

- To design a gripper with integrated sensors that can measure the grasping forces

Following the literature conclusions, the project aims to design a compliant gripper combined with either tactile sensors or curvature sensors (resistive strain sensors or optical fibers). The most important aspect of this project goal is to design with the integration of sensors in mind. Concerning the application in agri-food, a measurement of the grasping forces aims to cope with the deformable nature of the food products and the variation in size and shape. With a measurement of the force, it is desired to apply a force sufficiently high to grasp and hold the object, but sufficiently low such that it does not damage the object. Furthermore, a measurement of the force can help to deal with deviations in the world model of the object, which is often obtained by external cameras.

The envisioned functionality for a compliant gripper design with integrated sensors is as follows:

- Grasp objects of different shapes and sizes

- Measure the grasping forces, either directly or indirectly

Furthermore, there are some requirements to take into account when designing such a gripper:

- The sensors should not constrain the gripper performance

- The sensors and electronics should be shielded from the environment

- The sensor measurements should be sufficiently accurate

Bibliography

[1] David Richards, Timothy Sulser, and Keith Wiebe. World population day 2017: Ifpri models impact of population growth on demand for food, Jul 2017.

[2] Gert Kootstra, Xin Wang, Pieter M Blok, Jochen Hemming, and Eldert Van Henten. Selective harvesting robotics: current research, trends, and future directions. *Current Robotics Reports*, pages 1–10, 2021.

[3] C Wouter Bac, Eldert J van Henten, Jochen Hemming, and Yael Edan. Harvesting robots for high-value crops: State-of-the-art review and challenges ahead. *Journal of Field Robotics*, 31(6):888–911, 2014.

[4] Zhao De-An, Lv Jidong, Ji Wei, Zhang Ying, and Chen Yu. Design and control of an apple harvesting robot. *Biosystems engineering*, 110(2):112–122, 2011.

[5] Picknpack - flexible robotic systems for automated adaptive packaging of fresh and processed food products.

[6] Marco Controzzi, Christian Cipriani, and Maria Chiara Carrozza. Design of artificial hands: A review. *The Human Hand as an Inspiration for Robot Hand Development*, pages 219–246, 2014.

[7] Jun Shintake, Vito Cacucciolo, Dario Floreano, and Herbert Shea. Soft robotic grippers. *Advanced Materials*, 30(29):1707035, 2018.

[8] Jochen Hemming, C Wouter Bac, Bart AJ van Tuijl, Ruud Barth, Jan Bontsema, EJ Pekkeriet, and Eldert Van Henten. A robot for harvesting sweet-pepper in greenhouses. 2014.

[9] Festo. Festo multichoicegripper. Brochure, 2014.

[10] Dalibor Petković, Nenad D Pavlović, Shahaboddin Shamshirband, and Nor Badrul Anuar. Development of a new type of passively adaptive compliant gripper. *Industrial Robot: An International Journal*, 2013.

[11] Peter Steutel, Gert A Kragten, and Just L Herder. Design of an underactuated finger with a monolithic structure and largely distributed compliance. In *International Design Engineering Technical Conferences and Computers and Information in Engineering Conference*, volume 44106, pages 355–363, 2010.

[12] Jung-Yuan Wang and Chao-Chieh Lan. A constant-force compliant gripper for handling objects of various sizes. *Journal of Mechanical Design*, 136(7):071008, 2014.

[13] Lael U Odhner, Leif P Jentoft, Mark R Claffee, Nicholas Corson, Yaroslav Tenzer, Raymond R Ma, Martin Buehler, Robert Kohout, Robert D Howe, and Aaron M Dollar. A compliant, underactuated hand for robust manipulation. *The International Journal of Robotics Research*, 33(5):736–752, 2014.

[14] Chih-Hsing Liu, Chen-Hua Chiu, Ta-Lun Chen, Tzu-Yang Pai, Yang Chen, and Mao-Cheng Hsu. A soft robotic gripper module with 3d printed compliant fingers for grasping fruits. In *2018 IEEE/ASME International Conference on Advanced Intelligent Mechatronics (AIM)*, pages 736–741. IEEE, 2018.

[15] Daniela Rus and Michael T Tolley. Design, fabrication and control of soft robots. *Nature*, 521(7553):467–475, 2015.

[16] Panagiotis Polygerinos, Nikolaus Correll, Stephen A Morin, Bobak Mosadegh, Cagdas D Onal, Kirstin Petersen, Matteo Cianchetti, Michael T Tolley, and Robert F Shepherd. Soft robotics: Review of fluid-driven intrinsically soft devices; manufacturing, sensing, control, and applications in human-robot interaction. *Advanced Engineering Materials*, 19(12):1700016, 2017.

[17] Raphael Deimel and Oliver Brock. A novel type of compliant and underactuated robotic hand for dexterous grasping. *The International Journal of Robotics Research*, 35(1-3):161–185, 2016.

[18] Bianca S Homberg, Robert K Katzschmann, Mehmet R Dogar, and Daniela Rus. Robust proprioceptive grasping with a soft robot hand. *Autonomous Robots*, 43(3):681–696, 2019.

[19] Nicholas Farrow and Nikolaus Correll. A soft pneumatic actuator that can sense grasp and touch. In *2015 IEEE/RSJ International Conference on Intelligent Robots and Systems (IROS)*, pages 2317–2323. IEEE, 2015.

[20] Yu She, Chang Li, Jonathon Cleary, and Hai-Jun Su. Design and fabrication of a soft robotic hand with embedded actuators and sensors. *Journal of Mechanisms and Robotics*, 7(2), 2015.

[21] Hyung-Il Kim, Min-Woo Han, Sung-Hyuk Song, and Sung-Hoon Ahn. Soft morphing hand driven by sma tendon wire. *Composites Part B: Engineering*, 105:138–148, 2016.

[22] Eric Brown, Nicholas Rodenberg, John Amend, Annan Mozeika, Erik Steltz, Mitchell R Zakin, Hod Lipson, and Heinrich M Jaeger. Universal robotic gripper based on the jamming of granular material. *Proceedings of the National Academy of Sciences*, 107(44):18809–18814, 2010.

[23] Sukho Song, Carmel Majidi, and Metin Sitti. Geckogripper: A soft, inflatable robotic gripper using gecko-inspired elastomer micro-fiber adhesives. In *2014 IEEE/RSJ International Conference on Intelligent Robots and Systems*, pages 4624–4629. IEEE, 2014.

[24] Festo. Reliable and fast vacuum handling. Poster, 2006.

[25] Terabee. Time-of-flight principle. Blog, 2020.

[26] Linhan Yang, Xudong Han, Weijie Guo, Fang Wan, Jia Pan, and Chaoyang Song. Learning-based optoelectronically innervated tactile finger for rigid-soft interactive grasping. *IEEE Robotics and Automation Letters*, 6(2):3817–3824, 2021.

[27] Huichan Zhao, Kevin O'Brien, Shuo Li, and Robert F Shepherd. Optoelectronically innervated soft prosthetic hand via stretchable optical waveguides. *Science robotics*, 1(1):eaai7529, 2016.

[28] RS Pro. Alps alpine 15 pulse incremental mechanical rotary encoder with a 6 mm flat shaft. Website, 2022.

[29] Hossein Akbari et al. Proposing an index for qualitative comparison of six-axis force/torque sensors and optimization of maltese cross geometry to reduce cross-coupling error. *Modares Mechanical Engineering*, 17(10):153–164, 2018.

[30] Yousef Al-Handarish, Olatunji Mumini Omisore, Tobore Igbe, Shipeng Han, Hui Li, Wenjing Du, Jinjie Zhang, and Lei Wang. A survey of tactile-sensing systems and their applications in biomedical engineering. *Advances in Materials Science and Engineering*, 2020, 2020.

[31] Akihiko Yamaguchi and Christopher G Atkeson. Recent progress in tactile sensing and sensors for robotic manipulation: can we turn tactile sensing into vision? *Advanced Robotics*, 33(14):661–673, 2019.

[32] Siyuan Dong et al. *High-resolution tactile sensing for reactive robotic manipulation*. PhD thesis, Massachusetts Institute of Technology, 2021.

[33] Advait Jain, Marc D Killpack, Aaron Edsinger, and Charles C Kemp. Reaching in clutter with whole-arm tactile sensing. *The International Journal of Robotics Research*, 32(4):458–482, 2013.

[34] Sachin Chitta, Jürgen Sturm, Matthew Piccoli, and Wolfram Burgard. Tactile sensing for mobile manipulation. *IEEE Transactions on Robotics*, 27(3):558–568, 2011.

[35] Irin Bandyopadhyaya, Dennis Babu, Anirudh Kumar, and Joydeb Roychowdhury. Tactile sensing based softness classification using machine learning. In *2014 IEEE International Advance Computing Conference (IACC)*, pages 1231–1236. IEEE, 2014.

[36] PowerON. Touchdetect – tactile arrays and soft interfaces. Website, 2020.

[37] Zakriya Mohammed, Ibrahim Abe M Elfadel, and Mahmoud Rasras. Monolithic multi degree of freedom (mdof) capacitive mems accelerometers. *Micromachines*, 9(11):602, 2018.

Chapter 3

Research Paper

Indirect sensing method for contact location and force in a compliant finger

Rens de Rooij*

Abstract— **This paper presents a measurement method for a compliant gripper finger, whereby the location of the contact with an object and the exerted grasp force are measured indirectly, instead of directly on the contacting surface. For this purpose, the deformation is measured using strain gauges at two locations on the inside structure of the finger, where high deformations occur. The finger is modeled using a Finite Element Analysis, whereby strain data at the two sensor locations is gathered for a set of different contact locations. Now, by matching the measured data to a modeled scenario, both the actual contact location in this scenario and the accompanying contact force can be determined. For the experimental validation, the compliant finger embedded with the two strain gauges is manufactured and an experimental setup has been built. The results show that the contact location can be inferred from strain measurement and contact force is determined accurately up to order of magnitude of 10^{-1} newton. Comparing the force-deformation behavior of the original and the embedded finger, a maximum difference of 6% in actuation force was observed. Hence, the sensing method is useful to indirectly measure contact location and force for a compliant finger in contact with an object, while having a minor influence on the grasping performance of the original design.**

Keywords: Compliant gripper, interactive grasping, contact sensing, strain gauge, underactuation

I. INTRODUCTION

One of the challenges that humankind is currently encountering, is to provide all people with enough food [1]. The growing food demand, in combination with increasing labor shortages in agriculture [2], calls for automation in the agri-food industry. The number of robots in agriculture is growing, for example in the harvesting of fruits and vegetables [2] [3] [4] [5], and the processing of food products [6]. However, the amount of automation in agriculture and food processing is lagging behind other industries, where automation is widely used. An important challenge for robots handling food products is to prevent damage since these products are often deformable and fragile.

To overcome these challenges, new robotic grippers are developed that can handle natural products. For instance, compliant grippers are presented in [7], [8], [9], [10] and [11]. These grippers require only one actuator to grasp and are able to passively adapt to the shape of the grasped object due to the elastic deformation of their structure around the object. Besides being shape adaptable, they also provide soft and gentle contacts, and good force transferability due to predictable force-deflection behavior. At the same time, the undetermined compliant structure induces uncertainty about the stance of the compliant fingers and the exerted grasp forces. The addition of sensing to compliant grippers can present new possibilities to reduce this uncertainty and improve the grasping of natural products.

Embedding sensors in robotic grippers, so-called interactive grasping, provides feedback on the grasping process. The retrieved sensor data can be used to improve this grasping process, eliminate faulty grasps and obtain information about the grasped object. For example, tactile sensors placed on the contact surface of the gripper provide information about the interaction between gripper and object by directly measuring contact forces or contact locations [12] [13] [14]. A more indirect type of measurement is vision-based sensing, which comprises the placement of cameras or time-of-flight sensors on the end-effector, as in [5], to give visual feedback. Although sensors offer enhanced information about the grasping process, hardly any sensors are currently used in the end-effectors of industrial agricultural robotics for three main reasons. Firstly, the sensors will influence the grasping performance [12], especially when placed on the contact surface like tactile sensors. Secondly, environmental factors, like moisture and dirt, can easily influence the measurement, making the information unreliable. In the worst case, this can cause a breakdown of the fragile electronic components of the system. Thirdly, the operational space for integration of sensors in current robotic grippers is limited, and therefore installation is difficult.

Those problems can be solved by placing the sensors inside the finger's structure, instead of on the contact surface, implying indirect measurement of the interaction. Here is more space for installation and proper sensor placement. In addition, sensors are not in direct contact with the environment, and can therefore be more easily shielded from any outside disturbance. Instead of measuring directly on the contact surface, information about the number of interaction points, their locations, and the magnitude of the contact forces need to be established from measurable changes inside the structure of the finger. Proprioceptive sensing for example provides information on the positions and deformations of gripper fingers, by using rotational encoders, resistive strain sensors [15] [16] or optical fibers within the gripper [17] [18]. Compliant fingers are very suitable for this indirect sensing, due to their predictable force-deformation behavior. In contrast to rigid grippers, the deformation of a compliant finger strongly depends on the

* Authors are with the Faculty of 3mE, Delft University of Technology, The Netherlands.

external load on the finger and the location where this load is applied. The deformation or strain can be measured at any point on the structure of the finger, as the entire structure deforms under force, for example in the compliant finger in [9]. Consequently, this offers the possibility to determine the applied force and contact location by measuring strains at certain locations on the finger structure. The contact location provides insight into the gripper-object interaction, whereas the contact force is an important quantity for grasping, as it determines the stability of the grasp and the impact of the gripper on the object.

In this paper, we propose a method to estimate the contact location and force between a compliant finger and a rigid object based on strain measurement at discrete locations on the interior of the finger structure. The contact location estimate should be accurate enough to distinguish on which phalanges the contact takes place, while the contact force estimate should be accurate in order of magnitude of several newtons. In addition, the indirect sensing method will aim to minimize the impact of the sensors on the gripper performance in terms of mobility of the gripper and required actuation force.

The structure of the paper is as follows. In Section II, the compliant finger design and the indirect sensing method are presented, together with the Finite Element Analysis of the compliant finger where the force-strain behavior of the finger is established, and a description of the experimental set-up. In Section III the results of the experiments are shown, comprising the strain development in different load cases and the estimation of the contact forces. In Section IV the results are evaluated in detail to show the performance of the indirect sensing method, coupled with a discussion of the design choices and suggestions for future work. Section V presents the conclusions of the research.

II. Method

For the indirect sensing of the forces and contact location, a compliant gripper finger is combined with two strain gauges located on the internal structure of the finger. The strain development is expected to vary with the location where the finger is loaded, which is verified by constructing a Finite Element Analysis (FEA). The measured strains will be used to deduce the contact location, mainly distinguishing which phalanx contacts the object, and the contact forces, by matching the strain development to a simulated scenario.

An experimental set-up is then built containing a 3D-printed compliant finger with embedded strain gauges (Section II-C.1). To demonstrate the difference in strain development with varying contact phalanges, the finger is brought into contact with a disc. Hereby, the disc position with respect to the finger can be altered. At the same time, contact forces between the finger and a disc are measured.

A. Design of the finger with embedded strain gauges

1) Compliant finger: The specific compliant finger that is selected is based on the monolithic finger presented in

[9]. The proposed underactuated finger is shown in Fig. 1, whereby linear movement in direction of the red arrow is used to actuate the finger. Similar to human fingers, the compliant finger has three phalanxes that can be in contact with an object, counting from the base: 1 Proximal phalanx, 2 Middle phalanx, and 3 Distal phalanx. The finger is relatively simple due to the use of underactuation, with only one actuator required to perform the desired movement. Moreover, the open design of the finger leaves enough space for the placement of sensors in various locations on the internal structure.
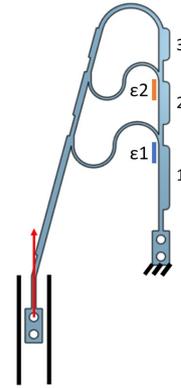
Fig. 1: Compliant finger

2) Strain gauges: Two strain gauges are placed on the internal structure of the compliant finger to measure the deformation upon actuation and loading, and deduce the contact location and contact forces. The strain gauges are indicated in Fig. 1 in blue (strain $\varepsilon 1$)and orange (strain $\varepsilon 2$). These sensors are easily available, have a high resolution, and can be installed easily. The strain gauges could be placed at various locations on the finger, but the locations indicated in Fig. 1 are selected for the high expected strains at these locations under different loading circumstances. As the strain development for just one sensor could be similar under different loading locations, two sensors are installed to be able to clearly distinguish between the contacting phalanges.

3) Finite Element Analysis: To simulate the deformations of the compliant finger under certain loads, a finite element model was created using COMSOL Multiphysics. The finger from Fig. 1 and the grasped object, modeled as a rigid disc, are analyzed with a 2-dimensional model. The position of the disc is varied in vertical and horizontal position to resemble different contact positions with the object. The deformations, stresses, and strains in the finger are evaluated, as well as the contact forces between finger and disc. Fig. 2 shows the distribution of Von Mises stresses in the finger, where in this case the middle phalanx of the finger contacts the rigid disc with an actuation displacement of 30 mm.

The simulation results were used to identify the two strain gauge locations, with relatively high strain under different loading circumstances. The strain development at these points was clearly distinct for varying contact posi-

Fig. 2: Von Mises stresses in the compliant finger when actuated in contact with a rigid disc. FEA simulation using COMSOL Multiphysics

Fig. 3: Schematic representation of the experimental set-up

tions and therefore served as the location for gluing the strain gauges when building the experimental set-up. The simulation results were also used to establish the expected relation between the strain in the finger and the contact forces between finger and disc, which will be the basis for deducing the contact forces from strain data.

B. Determination of contact location and contact force

To determine the contact location and the contact force between finger and disc in the horizontal direction, the FEA simulation is used. The FEA provides an estimate for the strain development and the contact forces for a known contact position. By varying the contact position, a large data set containing this strain and contact force development for different load cases is retrieved from the FEA. When the strain is measured in the finger, the strain development can be compared to the data set and thereby be matched to a simulated scenario. The accompanying contact position and contact forces in the horizontal direction for this simulated scenario can then be read out from the data set. The accuracy of this estimate is evaluated by comparing it to experimentally measured strain and contact forces for several contact positions.

C. Experimental validation

1) Experimental set-up: To evaluate the sensing method of measuring strain, and deducing the contact location and force accordingly, an experimental set-up was built. This set-up consists of one compliant finger with two strain gauges, a linear actuation mechanism, and a force sensor attached to a disc. Fig. 3 shows a schematic representation of the set-up. The experiments comprise the actuation of the finger against the disc, whereby the strain is measured on the locations indicated in red in Fig. 3, as well as the force on the disc in horizontal direction. A picture of the assembled set-up is shown in Fig. 4.
The details of the components in the experimental set-up:

Finger: The compliant finger is fabricated using 3D printing with TPC Flex 45 [19] flexible 3D printer filament.
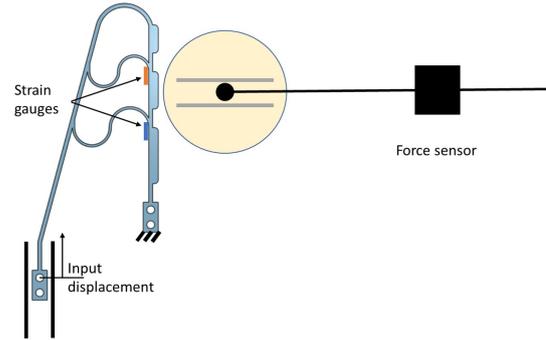
This material allows for large elastic deformations in the finger.

Strain gauges: The strain gauges used are standard linear strain gauges with a resistance of 120 Ω, produced specifically for use on deformable plastics (HBM, type 6/120 LY18 [20]). Two strain gauges are glued onto the compliant finger, on the locations indicated in Fig. 3. To correctly read out the sensors, the strain gauges are connected to three other strain gauges each, to form a Wheatstone bridge. These three reference strain gauges are placed on a block of the same material as the finger, in order to prevent thermal expansion of the material to influence strain measurements.

Actuation mechanism: The compliant finger is actuated using a linear input displacement. To achieve this input, the actuation end of the finger is placed on a linear guide and is actuated using a leadscrew connected to a stepper motor. This mechanism ensures strictly linear displacement with easily controllable speed and stroke.

Force sensor and disc: The final component of the experimental set-up exists of the force sensor attached to the disc. The force sensor is a FUTEK load cell with a measuring scope of up to 45 newtons. The sensor is limited to sensing force in one direction, and therefore loading in other directions is undesired. To the end that movement is only allowed in the force sensing direction, the disc is placed on a linear guide, perpendicular to the contact surface of the finger. Besides, the disc is allowed to rotate freely around its axis, to simulate frictionless contact with the finger.
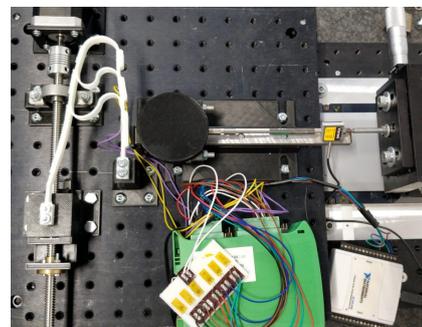
Fig. 4: Experimental set-up

2) Performed experiments: The performed experiments are aimed to relate the measured strain in the compliant finger to the location of contact and accompanying contact force between finger and disc in horizontal direction. Hereby, four main load cases are identified, varying in contact location of the finger with the disc: unloaded movement (no contact with disc), distal phalanx (highest phalanx in contact with disc), middle phalanx (as in Fig. 3) and proximal phalanx. Based on the FEA results it is expected that both the strain and the contact force in the horizontal direction increase linearly with increasing input displacement. The slopes of this linear increase differ per load case, for both the strain and contact force. Therefore, experiments are performed for all four load cases.

The disc is also placed at a distance from the finger, such that upon actuation the finger first deforms unloaded, then contacts the disc and is deformed around the disc. Hereby, the distinction between unloaded and loaded movement should be clearly visible in the strain development. This constitutes seven loading cases in total, shown in Table I.

TABLE I: Loading cases

Load case
Unloaded movement
Distal phalanx contact
Middle phalanx contact
Proximal phalanx contact
Initially no contact, then distal phalanx contact
Initially no contact, then middle phalanx contact
Initially no contact, then proximal phalanx contact

3) Impact of the sensors on gripper performance: Besides indirectly measuring contact information with sufficient accuracy, an important goal in this research is to minimize the impact of the sensors on the gripper performance. The main properties that constitute the performance of the compliant gripper finger are finger mobility and the actuation force. With this in mind, the addition of sensors should not lead to a restriction of the movement and deformation of the finger, or a significant increase in the force required to actuate the finger. To measure these properties, the compliant finger is manufactured twice in exactly the same manner, but for one finger, no strain gauges are attached. A visual inspection is performed on actuating both fingers to compare the mobility of the finger with and without sensors. Furthermore, the actuation force for both fingers is measured by slightly adjusting the experimental set-up.

III. RESULTS

The upcoming section shows the results of the experiments introduced in Section II. First, the strain development for the loading scenarios in Table I, is presented as measured with the strain gauges installed on the compliant finger, to demonstrate how different contact locations are distinguished. Then the performance of the contact force sensing is shown by comparing the contact force as acquired by the sensing method to the contact force measured in the experimental set-up. In addition, the performance of the finger with and

without strain gauges is observed and lastly, the occurrence of hysteresis is shown.

A. Different load cases

Fig. 5-8 display the strain development for the four main load cases: unloaded movement, distal phalanx contact, middle phalanx contact and proximal phalanx contact. The strain is measured upon an input actuation of up to 30 millimeters. Strain 1 ($\varepsilon1$, blue line) belongs to the lower strain gauge on the finger, whereas strain 2 ($\varepsilon2$, orange line) belongs to the upper strain gauge. The strain slopes differ per loading location. Consequently, by observing the slope, the phalanx in contact with the object can be determined. Fig. 9 and 10 display the variation in average strain slope per loaded phalanx, expressed in the change in strain per measuring time step. This variation is observed over multiple measurements, whereby the disc position is also varied over the length of the phalanx.
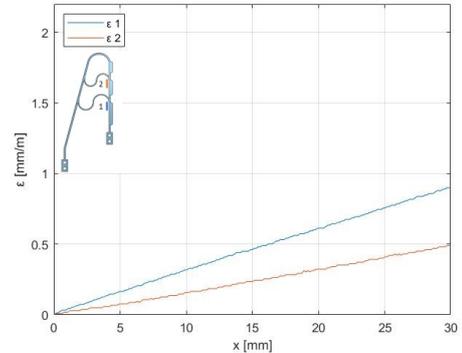
Fig. 5: Unloaded strain development
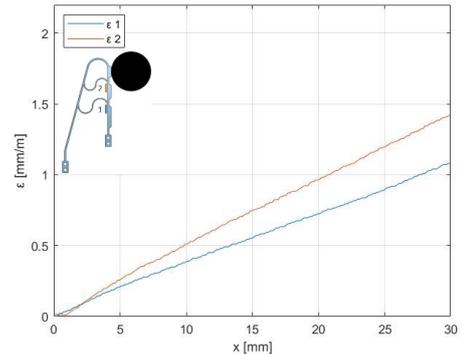
Fig. 6: Distal phalanx strain development

Fig. 11-13 show the strain development in case the disc is placed at a distance of 5 mm for the distal and middle phalanx and 3 mm for the proximal phalanx. In these cases, the finger initially deforms unloaded, with the strain slope comparable to the slope observed in Fig. 5. Then it contacts the disc at the indicated phalanx to continue deforming in a loaded manner, whereby the strain slope corresponds to the expected slope according to figures 9 and 10.
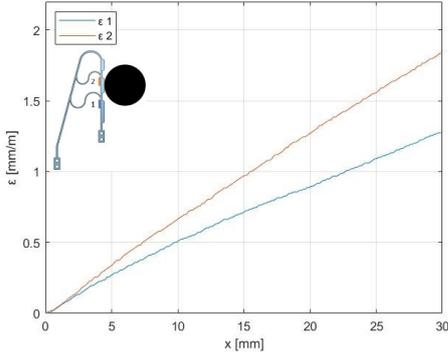
Fig. 7: Middle phalanx strain development
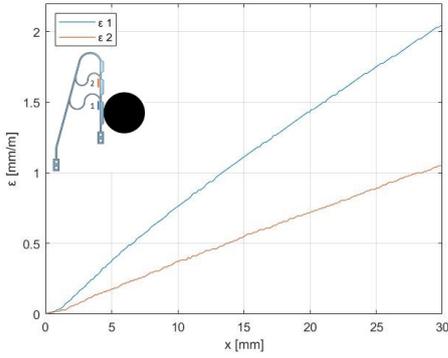
Fig. 8: Proximal phalanx strain development

B. Accuracy of contact force determination

To evaluate the performance of the sensing method, the general load cases from the previous section are tested multiple times with a force sensor attached to the disc, to measure the forces exerted by the finger on the disc. The contact forces in horizontal direction, as determined from the FEA model, are compared to these measured forces. Fig. 14 shows the force development for both cases, whereby the force at 30 mm input actuation is compared. The average error between the sensing method force and measured force is expressed in a percentage with respect to the total force and presented in Table II. The average error in determining the contact force for all load cases is 9 % (order of magnitude 10^{-1} newton), for total forces between 0.5 and 2.5 newton. The relative error is higher for small forces, while the absolute error is higher for larger forces, with a maximum error of 0.22 newton.

TABLE II: Error between modeled and measured contact force

Load case	Average error in force
Distal phalanx	11 %
Middle phalanx	10 %
Proximal phalanx	6 %
Distal phalanx, initially no contact	15 %
Middle phalanx, initially no contact	11 %
Proximal phalanx, initially no contact	0.5 %
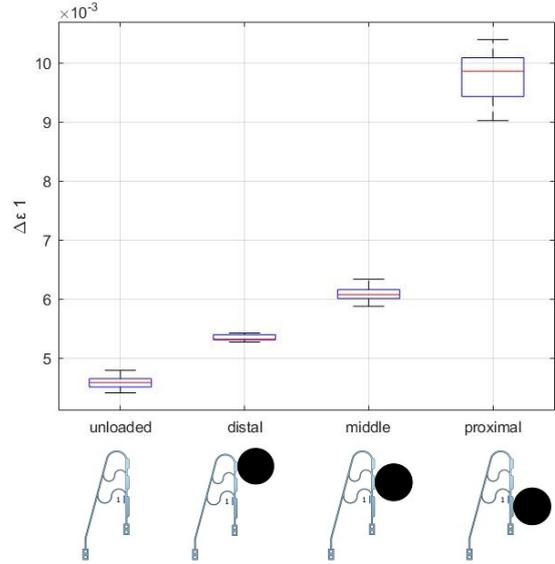
Fig. 9: Box plot showing the variation in average strain slope per load case for strain gauge 1
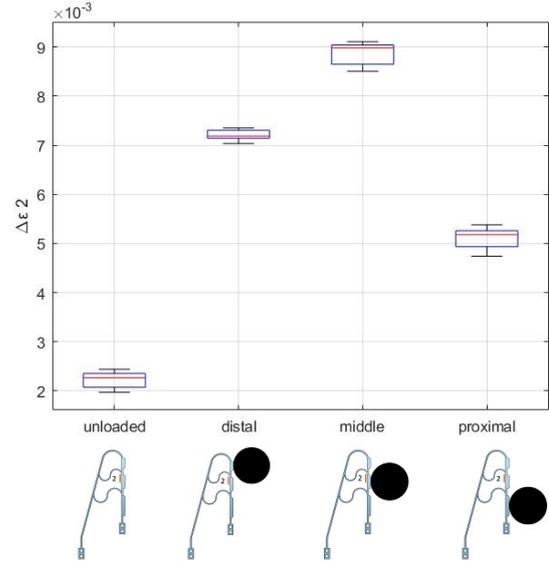
Fig. 10: Box plot showing the variation in average strain slope per load case for strain gauge 2

C. Impact of sensors on finger performance

As described in Section II-C.3, the impact of the sensors on the finger performance is measured in terms of mobility of the finger and required actuation force. The performance of the compliant finger with sensors is compared to a copy of the finger without sensors. Fig. 15 shows both fingers when fully actuated with a proximal phalanx load. A similar comparison is executed for the other load cases. Hereby, no significant difference is observed between the fingers when comparing the mobility through visual inspection.
The force required to actuate the finger in different load cases
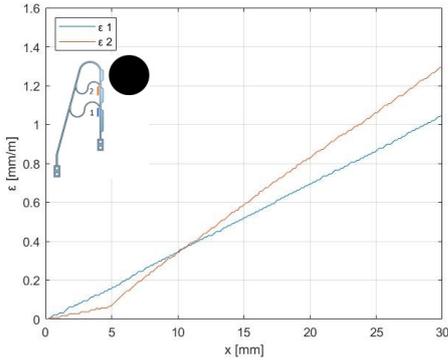
Fig. 11: Distal phalanx strain development, initially no contact with disc
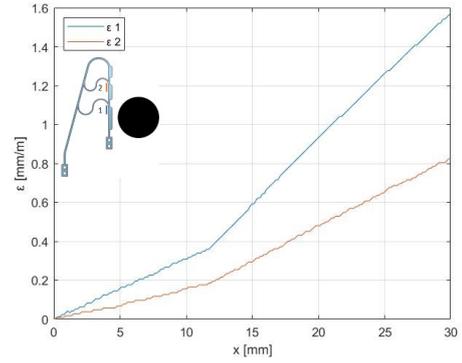
Fig. 13: Proximal phalanx strain development, initially no contact with disc
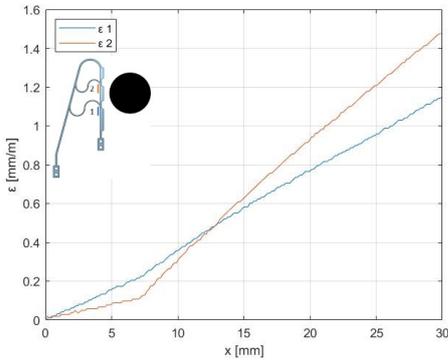
Fig. 12: Middle phalanx strain development, initially no contact with disc
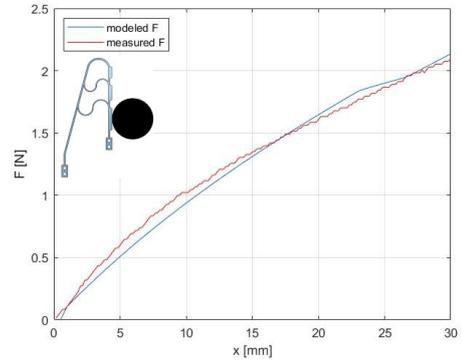
Fig. 14: Comparison between proximal phalanx force retrieved from simulation and directly measured force

for the finger with sensors and the finger without sensors is compared. The force is slightly higher for the finger with strain gauges on the structure, as presented in Table III, whereby the highest difference in force with respect to the original force is 6%.

TABLE III: Actuation force with/without sensors

Load case	Actuation force difference
Unloaded	0.05 N
Distal phalanx	0.07 N
Middle phalanx	0.07 N
Proximal phalanx	0.02 N

D. Hysteresis

During the experiments, some hysteresis is observed when looking at the full cycle of loading and unloading the finger. Both the strain and the contact force measurements display some hysteresis, as displayed in Fig. 16 and 17.

IV. DISCUSSION

A. Interpretation of the results

1) Contact location: Fig. 9 and 10 clearly indicate that by investigating the average strain slope, we can infer which phalanx is in contact with the disc, regardless of the exact location of contact on the phalanx. Moreover, we can also distinguish unloaded deformation from loaded deformation. These conclusions are supported by Fig. 11-13, where the strain in the unloaded part of the graphs complies with the expected strain slope for unloaded movement, whereas the strain in the second part complies to their respective contact phalanx.

However, the contact location distinction is limited to contact on one phalanx. When multiple phalanges are in contact with the object, the distinction based on strain slope no longer holds. When a load is applied on other parts of the finger than the phalanges, for example exerted by the environment of the object, then the present method can not determine the location of contact.

2) Contact force: Concluding from the results, the sensing method for indirectly measuring the contact forces has an average error of 9 % when compared to the force measurement in the experimental set-up, indicating the force measurement is accurate up to order of magnitude of 10^{-1} newton. The error is mainly caused by discrepancies between the FEA model and the set-up. Whereas the FEA model assumes an isotropic material for the compliant finger, the 3D-printed finger used in the experimental set-up is not isotropic. The fused deposition modeling technique
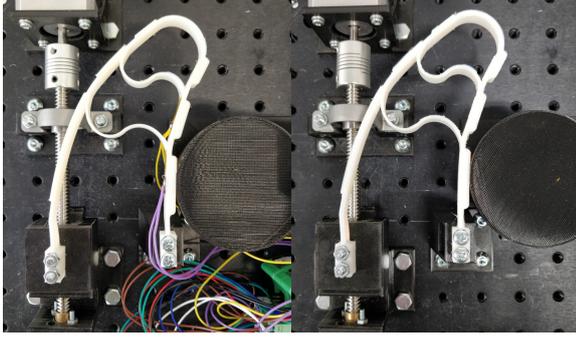
Fig. 15: Compliant finger with sensor (left) and without sensors (right), actuated with proximal phalanx load

Fig. 17: Hysteresis in proximal phalanx contact force measurement

Fig. 16: Hysteresis in proximal phalanx strain measurement

used in manufacturing the finger deposits the material layer by layer to build up the finger, leading to an anisotropic structure. The quality of the 3D print strongly depends on the settings of the printer. The material properties of the 3D printed finger will therefore differ from the FEA model. Besides the differences in material properties, the procedure for measuring the force differs as well. In the simulation, the contact force is modeled at the contact location. On the other hand, in the experimental set-up, the force sensor is attached to the linear guide upon which the disc is placed. A limitation to this method is the fact that only contact forces in the horizontal direction are considered. Although the horizontal force is dominant, forces in the vertical direction arise as well. Especially in cases with more than one phalanx in contact with the object, the vertical forces are significant. The FEA model is suitable to include these forces. However, the experimental set-up has to be adjusted to enable measurement of the vertical forces, in order to evaluate the FEA model.

B. Discussion of the design choices

The main design choices in this research are the selection of this specific compliant finger, the use of strain gauges as sensors and the location of the strain gauges. The combination of this compliant finger with strain gauges has both advantages and disadvantages. The behavior of the finger

was predictable, with both strain development and contact forces similar in simulation and experiments. The indirect sensing method ensures that the impact of the sensors on the performance is minimal, but there is a trade-off between sensing method accuracy and impact on finger performance. When comparing to literature, the indirect sensing method is less accurate in measuring contact location and forces than for example advanced tactile sensors. Similar accuracy might be achieved when measuring the actuation force and deducing the contact forces from this force, with minor impact on the finger performance as well. Nevertheless, force sensors and tactile sensors are more complex, harder to install, and less easily available than strain gauges.

The number of strain gauges was set on two to ensure that different loading scenarios can be distinguished. For the loading cases elaborated in this research, one strain gauge would have been sufficient to distinguish the loading scenarios, as can be concluded from the strain slope distinction in Fig. 9 and 10. However, when an increasing amount of loading scenarios is added, for example with multiple contact points between finger and disc, there might arise some overlap between scenarios when only using one strain gauge. In contrast, the use of one strain gauge instead of two will further reduce the impact on the finger performance.

The locations of the strain gauges are selected because of the large amount of strain expected at these locations under different loading cases. The strain gauges can be used to accurately measure smaller strains than observed in this research though, so several other locations on the finger can be considered. In further research, the strain gauge locations might be selected based on minimal influence on the gripper performance or ease of installation, instead of high expected strain.

As described in Section IV-A, the anisotropy of the material, as well as the quality of the 3D print will influence the performance of the sensing method. The material and manufacturing technique are selected for their availability and the possibility of rapid prototyping, but the success of the sensing method could greatly improve if the material properties are more accurately known and simulated in the

finite element model. The use of metals, in combination with more accurate manufacturing processes like Electrical Discharge Machining, can make a significant difference.

C. Impact of the sensors on finger performance

The results in Section III-C show that the influence of the sensors on the gripper performance is minimal. The force required to actuate the finger with sensors is up to 0.07 newton higher than the force for a finger without sensors, with a maximal relative increase of 6%. When comparing the stance of the fingers in the maximally actuated state, no significant differences are observed, indicating that the mobility and deformability of the finger are not influenced by the addition of the strain gauges. The force difference can be contributed to the fact that a strain gauge and soldering terminal for the wire connections are glued to the finger structure. This slightly increases the stiffness of the finger, resulting in an increased actuation force.

D. Hysteresis

When looking at the full cycle of loading and unloading the compliant finger in Fig. 16 and 17, both the strain and force graphs display some hysteresis. This hysteresis can have two causes: backlash in the mechanical components as the leadscrew and linear guide, and elastic hysteresis. Elastic hysteresis mainly occurs for elastomers and is caused by internal friction in the material. In the current experiments, the forces are evaluated during loading of the finger. When it is desired to evaluate the intermediate forces during unloading as well, the effects of hysteresis should be taken into account.

E. Future work

An obvious next step in this research would be to increase the number of measured scenarios. Varying the disc position in small steps over the entire length of the compliant finger and matching these load cases to simulated scenarios will provide further insight into the performance of this sensing method with respect to other sensing methods. Improving the FEA model such that it is more similar to the experimental set-up, for example by including the strain gauges in the simulation, will also benefit future research.

The method of using strain gauges and a simulation to determine contact location and force is not limited to this specific compliant gripper. In general, it could be applied to any comparable compliant gripper. Future work can verify that the method works accurately for different grippers as well, thereby demonstrating the general applicability of the sensing method. Moreover, combining the insights of the use on different grippers will help to improve the method.

The success of the current method for determining the force is dependent on the quality of the FEA model. Another method to deduce contact forces, that will eliminate this dependency, is calibration. Based on previous measurements, contact forces can be matched to the accompanying strain measurements by the use of algorithms. An example where force measurements are performed by calibration is presented in [17], for which optical fibers are used instead of strain gauges. The use of machine learning algorithms can help distinguish the different loading scenarios and further improve accuracy.

In this research, a single finger with sensors is evaluated. If several of these fingers were to be implemented into a gripper design, the measurements of the interaction between finger and object might improve the grasping process. For implementation in agri-food applications, it is important to shield the sensors though, to prevent breakdown due to environmental factors.

V. CONCLUSION

A sensing method is developed to distinguish different contact positions and indirectly measure contact forces in a compliant gripper finger by measuring the strain inside the finger structure. The method is implemented by manufacturing a compliant finger with two embedded strain gauges, and an experimental set-up was built to evaluate the method using experiments. The strain development for seven general contact scenarios is measured, whereby the strain slope is used to differentiate loaded and unloaded movement, and which phalanx is in contact with the object. The strain development is then matched to a modeled scenario in the FEA simulation. This model is used to determine the exact contact location and accompanying contact forces for the different scenarios. The experimental set-up is also used to measure the forces exerted by the finger on a disc, which are compared to the force values according to the sensing method. The sensed forces are reasonably accurate up to order of magnitude of 10^{-1} newton, whereby the limitation in accuracy is mainly caused by discrepancies between the FEA model and the manufactured finger. Furthermore, the impact of the sensors on the gripper performance is evaluated by comparing the mobility and actuation force for a finger with sensors and a finger without sensors, for different loading scenarios. When visually comparing, there is no difference observed in the mobility of the compliant finger. Only a marginal increase in actuation force of up to 0.07 newton (6%) is measured for the finger equipped with strain gauges, with respect to the same finger without sensors. Future research might study an increased number of load cases, as the current method only considers load on one phalanx. The use of a different material and fabrication technique could be investigated. Moreover, the indirect sensing method using strain gauges might be applied to other compliant fingers.

REFERENCES

[1] David Richards, Timothy Sulser, and Keith Wiebe. World population day 2017: Ifpri models impact of population growth on demand for food, Jul 2017.

[2] Gert Kootstra, Xin Wang, Pieter M Blok, Jochen Hemming, and Eldert Van Henten. Selective harvesting robotics: current research, trends, and future directions. *Current Robotics Reports*, pages 1–10, 2021.

[3] C Wouter Bac, Eldert J van Henten, Jochen Hemming, and Yael Edan. Harvesting robots for high-value crops: State-of-the-art review and challenges ahead. *Journal of Field Robotics*, 31(6):888–911, 2014.

[4] Zhao De-An, Lv Jidong, Ji Wei, Zhang Ying, and Chen Yu. Design and control of an apple harvesting robot. *Biosystems engineering*, 110(2):112–122, 2011.

[5] Jochen Hemming, C Wouter Bac, Bart AJ van Tuijl, Ruud Barth, Jan Bontsema, EJ Pekkeriet, and Eldert Van Henten. A robot for harvesting sweet-pepper in greenhouses. 2014.

[6] Wageningen University and Research. Picknpack - flexible robotic systems for automated adaptive packaging of fresh and processed food products.

[7] Dalibor Petković, Nenad D Pavlović, Shahaboddin Shamshirband, and Nor Badrul Anuar. Development of a new type of passively adaptive compliant gripper. *Industrial Robot: An International Journal*, 2013.

[8] Chih-Hsing Liu, Chen-Hua Chiu, Ta-Lun Chen, Tzu-Yang Pai, Yang Chen, and Mao-Cheng Hsu. A soft robotic gripper module with 3d printed compliant fingers for grasping fruits. In *2018 IEEE/ASME International Conference on Advanced Intelligent Mechatronics (AIM)*, pages 736–741. IEEE, 2018.

[9] Peter Steutel, Gert A Kragten, and Just L Herder. Design of an underactuated finger with a monolithic structure and largely distributed compliance. In *International Design Engineering Technical Conferences and Computers and Information in Engineering Conference*, volume 44106, pages 355–363, 2010.

[10] Lael U Odhner, Leif P Jentoft, Mark R Claffee, Nicholas Corson, Yaroslav Tenzer, Raymond R Ma, Martin Buehler, Robert Kohout, Robert D Howe, and Aaron M Dollar. A compliant, underactuated hand for robust manipulation. *The International Journal of Robotics Research*, 33(5):736–752, 2014.

[11] Raphael Deimel and Oliver Brock. A novel type of compliant and underactuated robotic hand for dexterous grasping. *The International Journal of Robotics Research*, 35(1-3):161–185, 2016.

[12] Akihiko Yamaguchi and Christopher G Atkeson. Recent progress in tactile sensing and sensors for robotic manipulation: can we turn tactile sensing into vision? *Advanced Robotics*, 33(14):661–673, 2019.

[13] Siyuan Dong et al. *High-resolution tactile sensing for reactive robotic manipulation*. PhD thesis, Massachusetts Institute of Technology, 2021.

[14] Sachin Chitta, Jürgen Sturm, Matthew Piccoli, and Wolfram Burgard. Tactile sensing for mobile manipulation. *IEEE Transactions on Robotics*, 27(3):558–568, 2011.

[15] Bianca S Homberg, Robert K Katzschmann, Mehmet R Dogar, and Daniela Rus. Robust proprioceptive grasping with a soft robot hand. *Autonomous Robots*, 43(3):681–696, 2019.

[16] Nicholas Farrow and Nikolaus Correll. A soft pneumatic actuator that can sense grasp and touch. In *2015 IEEE/RSJ International Conference on Intelligent Robots and Systems (IROS)*, pages 2317–2323. IEEE, 2015.

[17] Linhan Yang, Xudong Han, Weijie Guo, Fang Wan, Jia Pan, and Chaoyang Song. Learning-based optoelectronically innervated tactile finger for rigid-soft interactive grasping. *IEEE Robotics and Automation Letters*, 6(2):3817–3824, 2021.

[18] Huichan Zhao, Kevin O'Brien, Shuo Li, and Robert F Shepherd. Optoelectronically innervated soft prosthetic hand via stretchable optical waveguides. *Science robotics*, 1(1):eaai7529, 2016.

[19] RS PRO. Rs pro 1.75mm natural flex 45 3d printer filament. Website, 2023.

[20] HBM. Hbm strain gauges for experimental stress analysis. Website, 2023.

Chapter 4

Alternative method for determining contact forces: calibration

In the research paper in the previous chapter, the method for determining the contact forces comprises matching the experimentally measured strain development to a simulated scenario and reading out the accompanying contact force. An alternative method that was also implemented during the project is the use of calibration. In the upcoming sections, the method for performing a calibration of the strain to contact force in the compliant finger is described, based on experimental measurements.

4.1   Experimental measurements

As is established in the research paper, both strain and contact force in the compliant finger show an approximately linear increase upon increasing input displacement. The slope of the measured strain differs for the varying contact positions between finger and object. Therefore we can distinguish between contact on each of the three phalanges of the finger, based on the strain development. If these insights on the contact position are combined with the force measurements that are conducted using the experimental set-up, we can infer the expected force development for every contact position.

The experiments provide the strain and contact force development for a known contact position. The force development over increasing input displacement is approximately linear, so for a known contact position, the accompanying force slope can be read out from the measurements. This is visualized in figure 4.1, where the force development for proximal, middle, and distal phalanx contact is shown as measured in the experiments. The average force slope (ΔF) over time for a linear approximation, calculated using multiple measurements, is indicated in the figure.
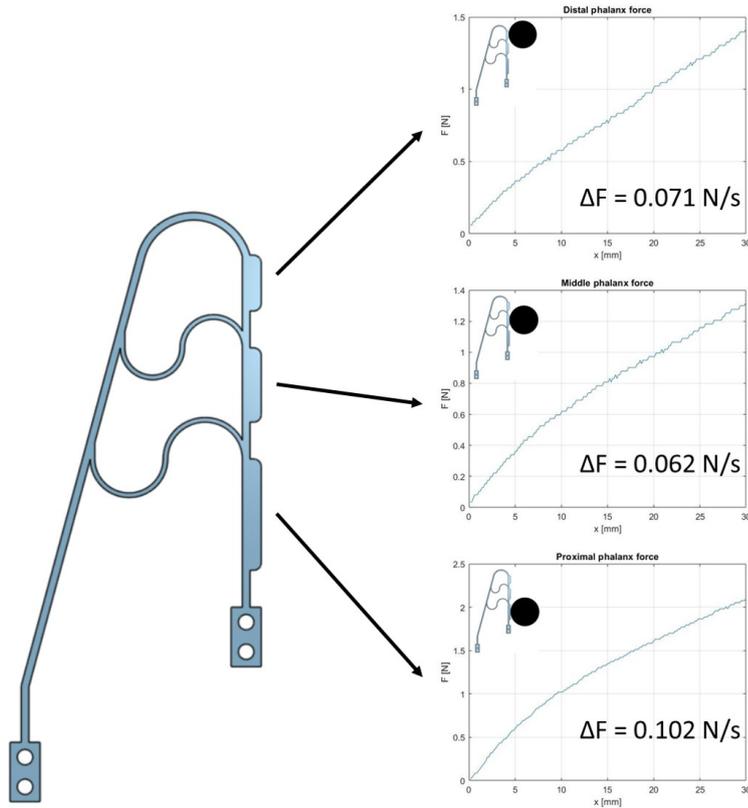
Figure 4.1: Force development for different contact locations as measured in the experimental set-up

4.2 Calculating contact forces

Now that the average force slope over time is established, based on experiments, and linearity is assumed, determining the loading time t is the last step towards calculating the contact forces accordingly using equation 4.1.

$$F = \Delta F * t \tag{4.1}$$

Granted that it is possible to distinguish the different contact locations from strain measurement, the loading time t can be inferred from the strain development over time. This is visualized in figure 4.2, where the strain development over time is plotted for the case that the disc is placed at a small distance from the finger. The first vertical red line in the figure indicates when actuation starts, followed by a period of unloaded deformation. The second red line indicates when the finger contacts the disc and loaded deformation starts. Consequently, the loading time t can be determined, indicated in the figure as well, and the force can be calculated using equation 4.1.

This method for calculating the expected contact force is implemented into an algorithm and applied to the strains measured during the experiments. The calculated force can then be compared to the force measured in the experimental set-up, to evaluate the accuracy of the calibration. These results are summarized in table 4.1, where the average error between calculated and measured force at full actuation is shown for the varying load cases, as a percentage of the total force. Figure 4.3 shows the comparison of a linear approximation of the force development according

to the calibration calculations, and the measured force development during an experiment. In this figure, the main cause of the errors in table 4.1 is visible, namely the fact that the linear approximation is not entirely accurate. Furthermore, the slopes in figure 4.1 are solely based on the average of previous experiments, so every experiment on its own will slightly diverge from this average.
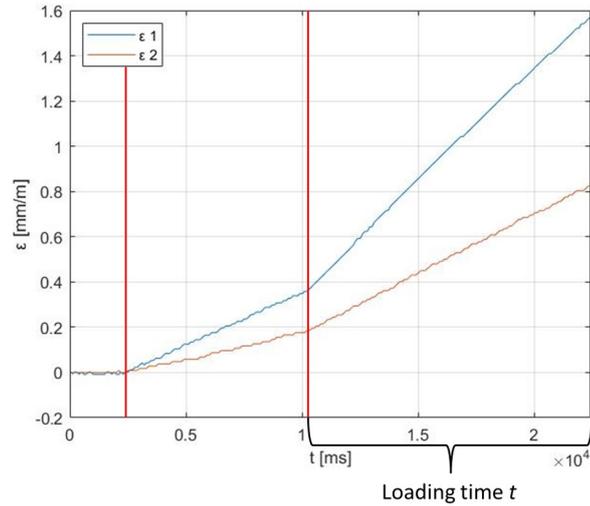
Figure 4.2: Proximal phalanx strain development, initially no contact with disc

Table 4.1: Error in contact force determination using calibration

Load case	Average error in force
Distal phalanx	5 %
Middle phalanx	4 %
Proximal phalanx	8 %
Distal phalanx, initially no contact	1 %
Middle phalanx, initially no contact	6 %
Proximal phalanx, initially no contact	16 %
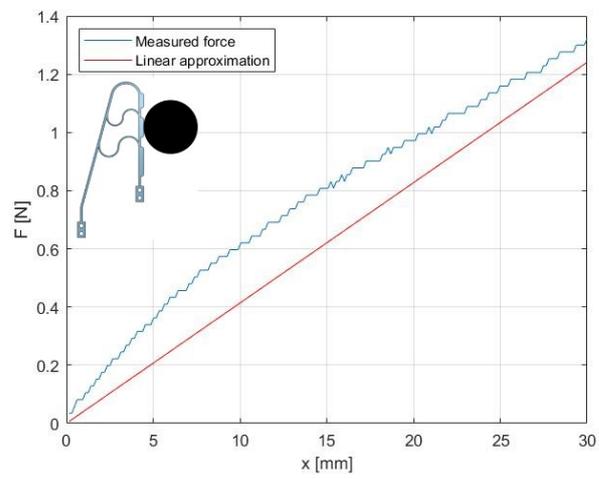
Figure 4.3: Middle phalanx force, measured and linear approximation according to calibration

Chapter 5

Discussion

This chapter will elaborate on the discussion part of the paper in chapter 3 and discuss the findings outside the scope of the paper. These are mainly some practical insights obtained throughout the project and more suggestions for future work.

5.1   Embedded strain gauges

The sensing method that was presented in the paper uses strain gauges as sensors for the deformation in the finger. To this end, the strain gauges are glued onto the backside of the structure of the finger, together with a soldering terminal where the wires of the sensor are connected. The gluing is done manually and is a careful and precise process, as the strain gauges need to be placed at the right location and straight aligned with the finger structure to ensure accurate measurements. In addition, the glue should not be spilled on other parts of the structure, for it could cause undesired restrictions to the deformation of the finger. The soldering should be performed carefully as well, to make sure the wires are well connected, while at the same time making sure the structure is not heated excessively.

In further research, some of these operations might be altered to take away the challenges and inaccuracy involved in the manual actions. For example, the shape of the strain gauges can be integrated into the finger design, such that they can be fitted in exactly one way. This will ensure straight placement at the right location. An even more accurate process would be to fully embed the sensors in the finger during manufacturing. An example of such a process can be found in [2], where a sensor is fully embedded inside a soft robotic finger during a casting process.

For the prototype that was used in this research, the strain gauges and connected wires were placed on the outside, without any shielding or integration into the structure. When future research would consider implementing several of these fingers into a complete gripper design, it is imperative to properly integrate the sensors and wiring into the finger structure, for they should not restrict gripper performance in any way. Moreover, when the application into agri-food processes is studied, the sensors and wiring should not be exposed to dirt or humidity coming from the environment, to prevent breakdown.

5.2 Plastic deformation in the compliant finger

The experimental measurements described in the paper were conducted for multiple prototype fingers, with only the results for the final prototype presented in the paper. During measurement with one of the early prototypes, the significant influence of small plastic deformations on the measurements was observed. Some spilled glue from the strain gauges and a small plastic deformation affected the finger's structure and deformability. As a consequence, the measured strain diverged from the expected strain development according to the FEA. This is visualized in figure 5.1, where strain $\varepsilon 0$ is higher than $\varepsilon 1$ for the prototype, while in simulation the strain development is clearly different with $\varepsilon 1$ higher than $\varepsilon 0$. Besides the strain, the contact forces measured in the experiments also diverged due to the increased stiffness of the finger as a result of the plastic deformation, with higher forces required to deform the finger. In addition, for similar measurements, the forces increased over time, probably due to strain hardening.

To prevent such disturbances in future research, careful handling of the compliant fingers in order not to induce plastic deformations is critical. Alternatively, materials could be used that are more resilient to plastic deformation.
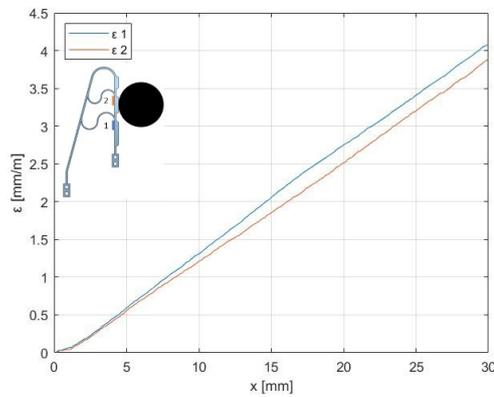
(a) Middle phalanx strain, early prototype finger
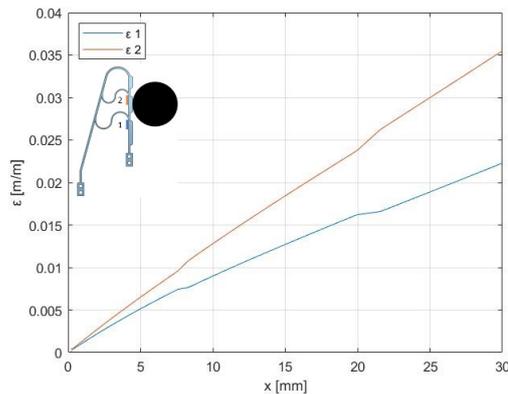
(b) Middle phalanx strain retrieved from simulation

Figure 5.1: Strain development comparison between deformed early prototype finger and simulation

41

Chapter 6

Conclusion

In this thesis, the addition of sensing to robotic grippers is investigated. Through a literature study existing gripper principles are analyzed, as well as sensing methods that can be utilized for grasping purposes. This study results in an overview of the possibilities of combining gripper principles with certain sensing methods, as well as an analysis of the challenges of embedding sensors in grippers. The results and insights from the literature study lead to the main research question: can we estimate the contact location and contact force between a compliant finger and an object indirectly by measuring the strain inside the structure?

As described in chapter 3, a sensing method is developed to distinguish different contact positions and indirectly measure contact forces in a compliant gripper finger by measuring the strain inside the finger structure. The method is implemented by manufacturing a compliant finger with two embedded strain gauges, and an experimental set-up was built to evaluate the method using experiments. The strain development for seven general contact scenarios is measured, whereby the strain slope is used to differentiate loaded and unloaded movement, and which phalanx is in contact with the object. The strain development is then matched to a modeled scenario in the FEA simulation. This model is used to determine the exact contact location and the accompanying contact forces for the different scenarios. The experimental set-up is also used to measure the forces exerted by the finger on a disc, which are compared to the force values according to the sensing method, whereby the sensed forces are reasonably accurate up to order of magnitude of 10^{-1} newton. Furthermore, the impact of the sensors on the gripper performance, as evaluated by comparing the mobility and actuation force for a finger with sensors and a finger without sensors, is minimal.

These results show that the addition of sensors to robotic gripper fingers can provide accurate measurements of quantities that are critical in grasping, without having a significant impact on the gripper performance. Future research has to determine whether the sensing method can be implemented into other compliant finger designs, and whether the measured quantities may help to improve grasping processes when multiple fingers are integrated into a complete gripper design.

Appendix A

Experimental set-up

The experimental set-up was built to verify the sensing method of measuring strain and deducing the contact location and force. This section contains an extensive description of the components of the set-up. The set-up consists of one compliant finger with two strain gauges, a linear actuation mechanism and a force sensor attached to a disc, placed on a linear stage. Figure A.1 shows a schematic representation of the set-up. The experiments comprise the actuation of the finger against the disc, whereby the strain is measured on the locations indicated in red in figure A.1, as well as the force on the disc in horizontal direction. The entire set-up is installed on a platform to ensure all components are firmly set and distances between components are fixed.
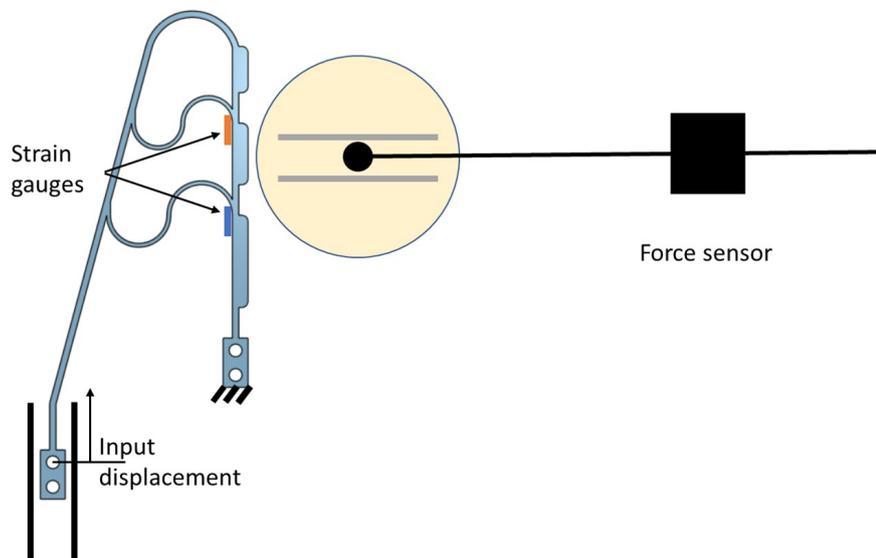
Figure A.1: Schematic representation of the experimental set-up

A.1 Compliant finger

The compliant finger that is selected as a prototype is based on the monolithic finger presented in [1]. The design is altered to make it more suitable for manufacturing by 3D printing. The dimensions of the Computer-Aided Design (CAD) model are shown in figure A.2 and table A.1, whereby the out-of-plane thickness of the finger will be 10 mm. The CAD model is then fabricated using a standard fused deposition modeling 3D printing technique with TPC Flex 45[3] flexible 3D printer filament. This material allows for large elastic deformations in the finger.
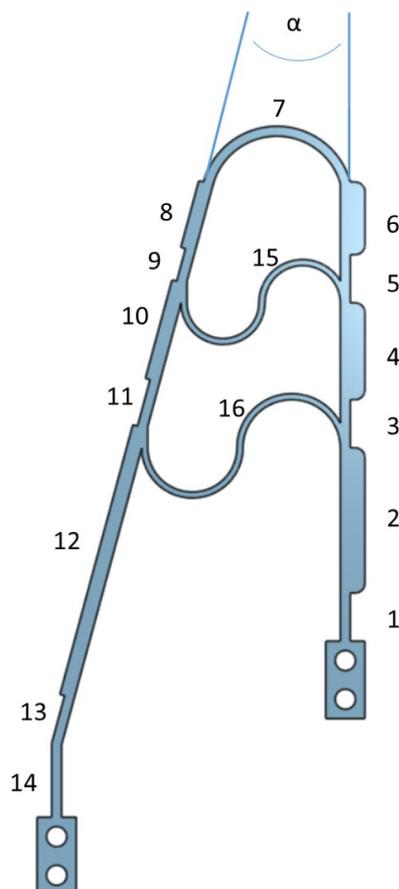
Figure A.2: Finger segments

Table A.1: Finger dimensions

Segment	1	2	3	4	5	6	7	8	9	10	11	12	13	14	15	16
Length (mm)	10	30	10	20	10	15		14	7	21	10	58	10	15		
Thickness (mm)	2	5	2	5	2	5	2	3	2	3	2	3	2	2	1.2	1.2
Angle α (rad)							$\pi/12$									

A.2   Strain gauges

Two strain gauges are installed on the compliant finger to measure the deformation. The strain gauges used are standard linear strain gauges with a resistance of 120 Ω, produced specifically for use on deformable plastics (HBM, type 6/120 LY18[4]). The sensors require some circuitry and calibration to function properly. This circuitry and the calibration calculations are presented in this section.

Strain gauge circuit

Strain ε is a measure for the deformation of a material, usually represented as the change in length Δl relative to the original length l_0.

$$\varepsilon = \frac{\Delta l}{l_0} \tag{A.1}$$

In a strain gauge, this change in length is perceived as a change in electrical resistance. This ΔR is related to the strain through equation A.2, whereby k is the gauge factor as provided by the strain gauge producer.

$$\frac{\Delta R}{R_0} = k\varepsilon \tag{A.2}$$

The strain gauge is implemented in an electrical circuit, such that the change in resistance can be read out. Changes in resistance are commonly read out using a Wheatstone bridge circuit, as shown in figure A.3. The change in resistance results in a voltage difference in the bridge, which is measured using a voltage meter. In this case, all four resistances indicate strain gauges. The upper right strain gauge is placed on the compliant finger, the other three are placed on a block of the material that the finger is made of. The reason for this is to prevent thermal expansion of the material to influence the strain measurement. Although thermal expansion can still deform the material, the deformation is equal for the reference strain gauges in the Wheatstone bridge as these are placed on the same material. As two strain gauges will be installed on the compliant finger, two complete Wheatstone bridge circuits are required.
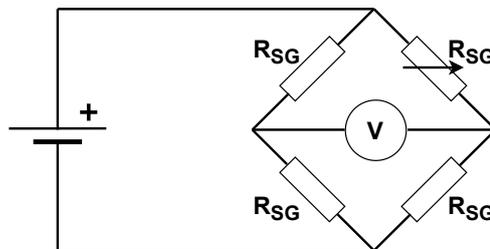
Figure A.3: Wheatstone bridge circuit

Calibration calculations

Using the Wheatstone bridge circuit, a voltage difference ΔV is measured upon application of strain to the strain gauge on the compliant finger. Calibration is required to investigate the amount of strain that leads to a certain voltage difference. To achieve this calibration, a shunt resistor of known resistance is placed in parallel with the strain gauge on the finger, as shown in the circuit in figure A.4. This leads to a voltage difference. The calculations in A.3 show how the

strain - voltage difference relationship is established, while table A.2 contains the variables used in the calculations. This calculation is performed twice, for both strain gauges that are placed on the compliant finger. The outcome of the calculation is then used to convert the measured voltage signal into a strain.
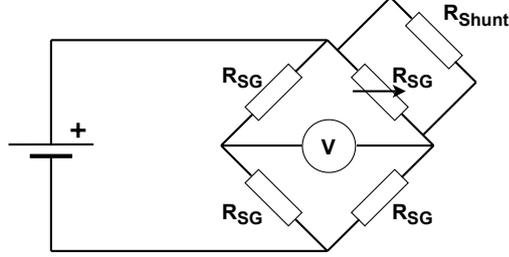
Figure A.4: Wheatstone bridge circuit with shunt resistor for calibration

Table A.2: Variables in the calculations

Symbol	Name	Units
ΔV	Voltage difference	V
R_{SG}	Strain gauge resistance	Ω
R_{shunt}	Shunt resistance	Ω
R_v	Resistance of strain gauge and shunt in parallel	Ω
k	Gauge factor	-
ε	Strain	m/m
CF	Conversion factor voltage to strain	m/m/V

$$
\begin{aligned}
\frac{1}{R_v} &= \frac{1}{R_{SG}} + \frac{1}{R_{shunt}} \\
R_v &= \frac{R_{SG} * R_{shunt}}{R_{SG} + R_{shunt}} \\
\Delta R &= R_{SG} - R_v \\
\varepsilon &= \frac{\Delta R}{R_{SG} * k} \\
CF &= \frac{\varepsilon}{\Delta V}
\end{aligned}
\tag{A.3}
$$

A.3   Actuation mechanism

The compliant finger is actuated using a linear input displacement. To achieve this input, the actuation end of the finger is placed on a small linear guide and is actuated using a leadscrew connected to a stepper motor. This mechanism ensures strictly linear displacement with easily controllable speed and stroke. Figure A.5 shows the actuation mechanism including the finger as it was designed using CAD.

The stepper motor is a standard NEMA17 stepper motor, that is connected to the leadscrew through a flexible motor coupling. The leadscrew and leadscrew nut have a lead of 2 mm, so upon
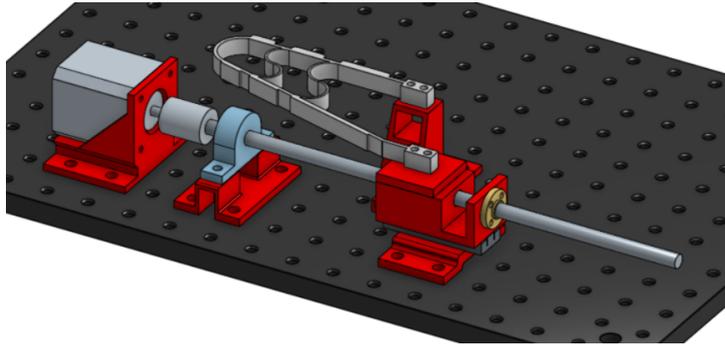
Figure A.5: Actuation mechanism as in the CAD model

a 360° motor rotation, the finger is actuated with a 2 mm input displacement. The leadscrew is supported by a ball bearing, shown in blue in figure A.5, whereas the red parts in the figure are all custom-designed parts that are 3D printed in polylactic acid (PLA). The stepper motor is controlled using an Arduino Uno and L298N motor driver module. Hereby, the motor speed is set at 45 rpm and the motor output at 15 full rotations. With the 2 mm lead of the leadscrew, this results in a linear displacement of 30 mm for the actuation side of the finger with a constant speed of 1.5 mm per second.

A.4   Force sensor, disc and linear stage

The last component of the experimental set-up exists of the force sensor attached to the disc. The force sensor is a FUTEK load cell with a measuring scope of up to 45 newtons. The sensor is limited to sensing force in one direction, and therefore loading in other directions is undesired. The disc is placed on a linear guide to only allow movement in the force-sensing direction, perpendicular to the contact surface of the finger. The linear guide exists of a rail connected to the set-up platform and a cart on the rail. The force sensor can be connected to this cart. The disc axis is placed in a ball bearing, such that the disc is allowed to rotate freely around its axis. The ball bearing is in turn installed on the linear cart. The free rotation of the disc when in contact with the compliant finger is realized to simulate frictionless contact between disc and finger. Figure A.6a shows the CAD model of the disc installed on the linear cart, with the red parts again custom-designed parts that are 3D printed in PLA. Figure A.6b shows how the force sensor is connected to the cart on the linear rail.
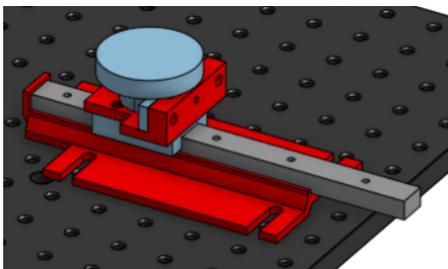
(a) CAD model of the disc on the linear rail
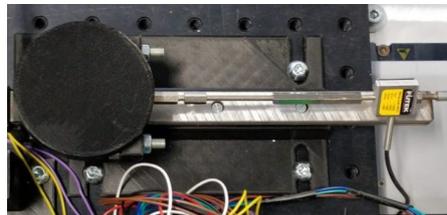
(b) Picture of the force sensor(right) connected to the linear cart

Figure A.6: Linear stage and force sensor

Appendix B

Finite Element Analysis in COMSOL Multiphysics

For the finite element analysis, COMSOL Multiphysics was used. A 2-dimensional model of the compliant finger in contact with a rigid disc is simulated using the solid mechanics physics in COMSOL.

B.1   Model set-up

Solid mechanics is selected as the physics, in combination with a stationary study. A 3-dimensional CAD model of the compliant finger is loaded into COMSOL as geometry, for which a cross section is taken to obtain the desired 2D representation. A circle is added to represent the disc. The entire 2D geometry is given an out-of-plane thickness of 10 mm, the same thickness as the 3D-printed prototype compliant finger. The geometry is shown in figure B.1. As the exact material that is used to manufacture the prototype is not available in COMSOL, a thermoplastic polyurethane is selected and the material properties are altered such that they are equal to the properties as provided by the 3D-print material producer [3]. The disc material is arbitrarily chosen to have a relatively much higher resistance to deformation than the finger. A contact pair is established between the disc geometry and the surface of the phalanges of the compliant finger. Within the solid mechanics tab, the disc is defined as a fixed domain, whereas the base of the finger is fixed and on the actuation side a strictly linear input displacement is defined. An extra fine mesh is selected to be able to accurately simulate the contact mechanics.

B.2   Simulation and results

For the stationary study, an auxiliary sweep is defined for the input displacement parameter, so that the input is incrementally increased from 0 to 30 millimeters. For different simulations, the disc position with respect to the finger is varied, both in height and in initial distance from the finger. The results that are obtained for these simulations are mainly focused on stress and deformation in the finger, and contact forces between finger and disc. 2-dimensional images are retrieved showing the stress distribution in the finger for every input displacement step, as well as the contact force and location of contact between finger and disc (shown in figure B.2).
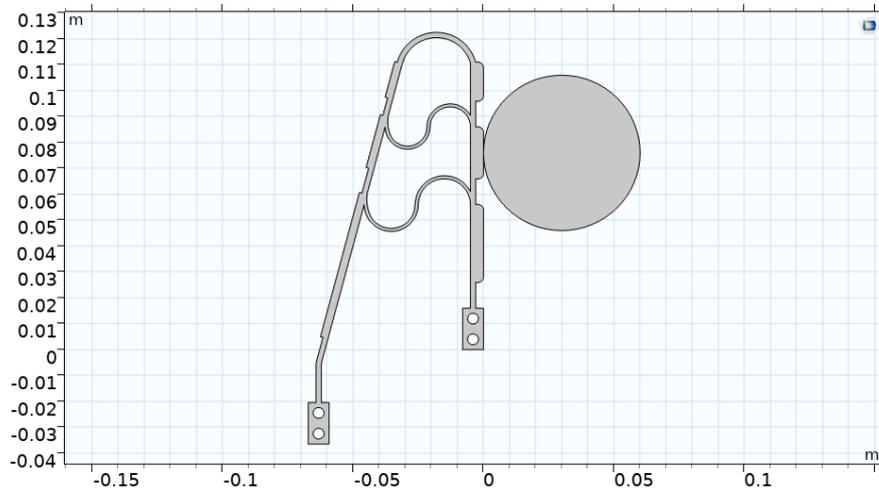
Figure B.1: 2-dimensional geometry used in the finite element analysis in COMSOL Multiphysics

Furthermore, the strain development at several points in the finger is plotted against the input displacement. The total contact force in the model, both in the x- and y-direction, is plotted against the input displacement as well.
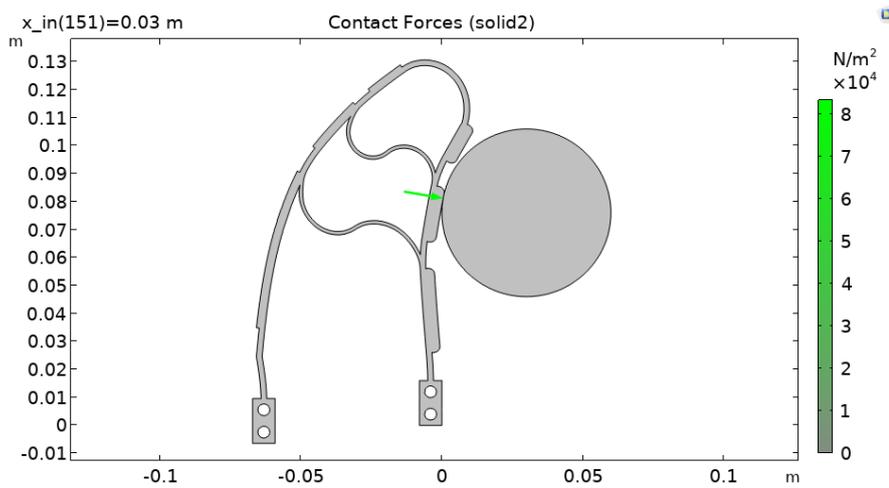
Figure B.2: Contact pressure and location of contact between finger and disc upon an input actuation of 30 mm. FEA simulation using COMSOL Multiphysics

Bibliography

[1] Peter Steutel, Gert A Kragten, and Just L Herder. Design of an underactuated finger with a monolithic structure and largely distributed compliance. In *International Design Engineering Technical Conferences and Computers and Information in Engineering Conference*, volume 44106, pages 355–363, 2010.

[2] Bianca S Homberg, Robert K Katzschmann, Mehmet R Dogar, and Daniela Rus. Robust proprioceptive grasping with a soft robot hand. *Autonomous Robots*, 43(3):681–696, 2019.

[3] RS PRO. Rs pro 1.75mm natural flex 45 3d printer filament. Website, 2022.

[4] HBM. Hbm strain gauges for experimental stress analysis. Website, 2022.